The Mathematics of Ethylene Oligomerisation and Polymerisation

Craig T. Young[1] · Richard von Goetze[1] · Atanas K. Tomov[1] · Francesco Zaccaria[1] · George J. P. Britovsek[1]

Abstract

Linear α-olefins or LAOs are produced by the catalytic oligomerisation of ethylene on a multimillion ton scale annually. A range of LAOs is typically obtained with varying chain lengths which follow a distribution. Depending on the catalyst, various types of distributions have been identified, such as Schulz–Flory, Poisson, alternating and selective oligomerisations such as ethylene trimerisation to 1-hexene and tetramerisation to 1-octene. A comprehensive mathematical analysis for all oligomer distributions is presented, showing the relations between the various distributions and with ethylene polymerisation, as well as providing mechanistic insight into the underlying chemical processes.

Keywords Ethylene · Alpha-olefins · Oligomerisation · Mathematics · Distribution · Recurrence

1 Introduction

Linear alpha olefins (LAOs, or 1-alkenes) find extensive use as co-monomers in olefin polymerisation and as intermediates to detergents, lubricants, and plasticisers [1–3]. Global consumption of LAOs grew at an average annual rate of 5.6% from 2012 to 2016, and global capacity for LAO production has been estimated at 6.2 million tonnes per year (mtpy) for 2018 [4, 5]. LAOs are generally prepared via the oligomerisation of ethylene, as is shown below in Scheme 1 [6].

LAO processes may be grouped into two types: wide-range and on-purpose [7]. Wide-range processes give a distribution of LAO products from C_4 to C_{20+}, whilst on-purpose processes predominantly give C_4, C_6 or C_8 LAOs [7]. Examples of catalytic systems used in industry are given in Figs. 1 and 2 [6–9].

Three of the most common types of distributions from ethylene oligomerisation and polymerisation processes—namely Schulz–Flory, selective-LAO, and Poisson—are observed with the systems in Figs. 1 and 2. In addition, a number of alternating LAO distributions with chromium-based systems have been reported in the literature [11–17]. These four types of ethylene product distribution are depicted in Fig. 3.

Following on from the ground-breaking work 80 years ago by Schulz and Flory [18, 19], novel mathematical approaches for analysing product distributions from ethylene oligomerisation and polymerisation processes are presented in this paper. These approaches provide straightforward, applicable methods for characterising key mechanistic features of underlying catalytic processes, and demonstrate how Schulz–Flory, alternating, selective-LAO, and Poisson distributions may be considered as parts of a connected product distribution landscape.

2 Modelling Steady-State Oligomerisation Processes

2.1 First-Order Oligomerisation Processes

In 1935, Schulz characterised the mathematics behind first-order oligomerisation processes [18]. He noted the direct proportionality between $mol(n)\%$ (mol percentage for an oligomer of n ethylene units) and the product of a sequence featuring a constant propagation probability α:

$$mol(n)\% = c_1\alpha^n \tag{1a}$$

✉ George J. P. Britovsek
g.britovsek@imperial.ac.uk

1 Department of Chemistry, MSRH Imperial College London, 80 Wood Lane, London W12 0BZ, UK

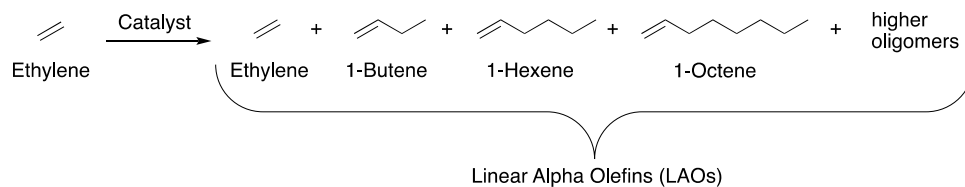**Scheme 1** Generic scheme for LAO synthesis via the oligomerisation of ethylene

Fig. 1 Wide-range industrial processes giving LAO distributions from C_4 to C_{20+} (X = appropriate anion). Note: INEOS's process gives a Poisson distribution of LAOs, whilst the SHOP and Gulfene processes give Schulz–Flory distributions of LAOs
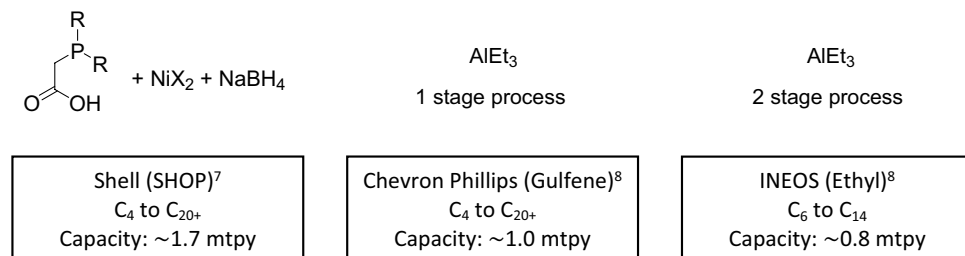

Fig. 2 On-purpose industrial processes predominantly giving C_4, C_6 or C_8 LAOs (X = appropriate anion)
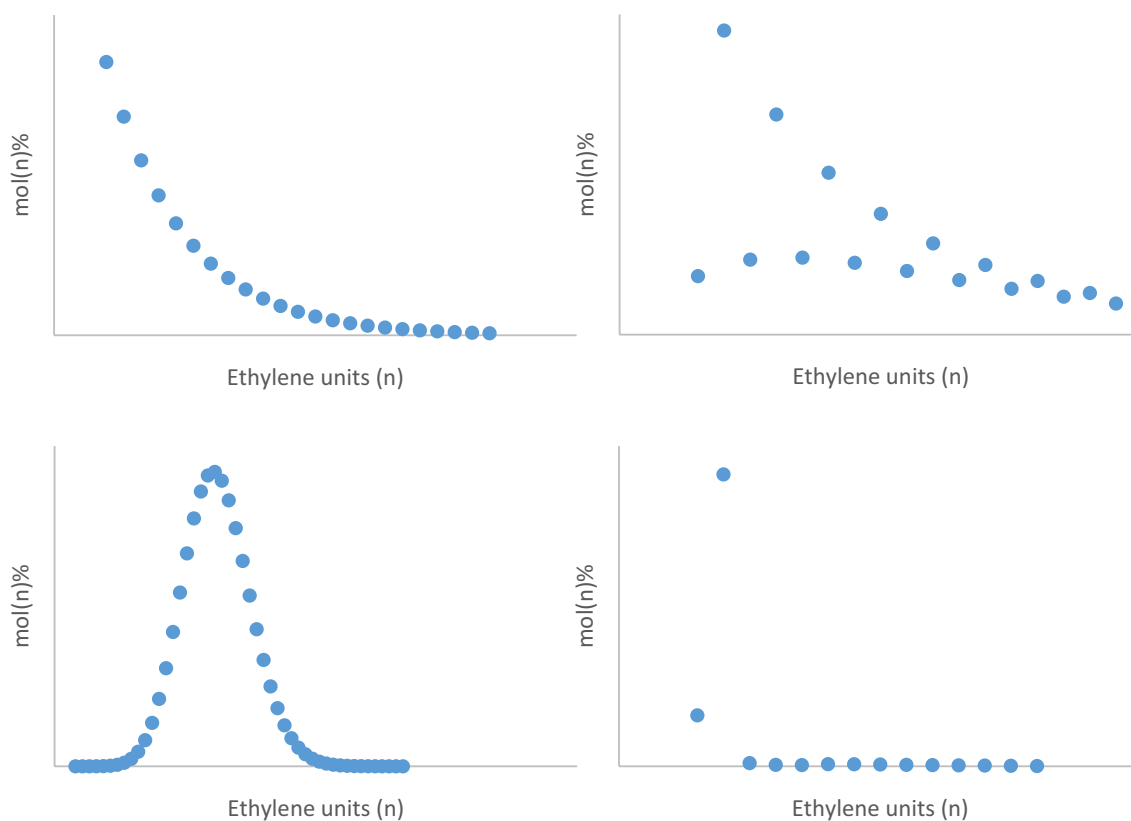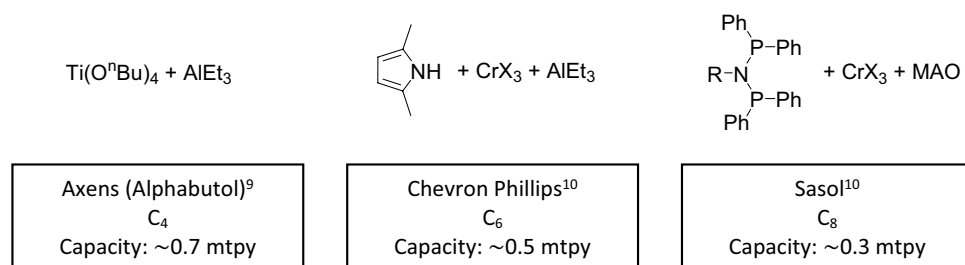

Fig. 3 Clockwise from top-left: illustrations of Schulz–Flory, alternating, selective-LAO, and Poisson distributions

Following a *continuous function approximation*, this implies (see SI.1.1 for derivation):

$$mol(n)\% = -(\ln \alpha)\alpha^n \tag{1b}$$

The relationship between $wt(n)\%$, $mol(n)\%$ and n is:

$$wt(n)\% \propto mol(n)\%(RFM\,C_2H_4)n \tag{2a}$$

where (RFM C_2H_4) is the Relative Formula Mass of ethylene.

Using the expression for $mol(n)\%$ from Eq. 1a and condensing:

$$wt(n)\% = c_2 n\alpha^n \tag{2b}$$

Again making use of a continuous function approximation (see SI.1.2 for derivation), this implies:

$$wt(n)\% = (ln\alpha)^2 n\alpha^n \tag{2c}$$

The following year, in 1936, Flory presented precise derivations without making use of continuous function approximations [19]. Flory noted the dependence of $mol(n)$, the amount of moles for each oligomer of n ethylene units, on the product of $(n-1)$ propagation steps and 1 elimination step along with R, the total mol of oligomers produced during the reaction time:

$$mol(n) = (1 - \alpha)\alpha^{n-1}R \tag{3a}$$

Consequently:

$$mol(n)\% = \frac{(1 - \alpha)\alpha^{n-1}R}{R} = (1 - \alpha)\alpha^{n-1} \tag{3b}$$

It follows that:

$$wt(n) = n(RFM\,C_2H_4)mol(n) = n(RFM\,C_2H_4)R(1 - \alpha)\alpha^{n-1} \tag{4a}$$

which gives (see SI.1.3 for derivation):

$$wt(n)\% = n(1 - \alpha)^2\alpha^{n-1} \tag{4b}$$

Comparing Eq. 1b with Eq. 3b, it is evident that both Schulz's equation and Flory's equation express:

$$mol(n)\% = c\alpha^n \tag{5a}$$

The two Eqs. 1b and 3b are subtly different, as shown in Fig. 4, because $-(ln\alpha)$ is the proportionality constant for Schulz and $(1 - \alpha)/\alpha$ is the proportionality constant for Flory. However, in practice, this makes little difference because α is typically determined by taking natural logarithms to each side of Eq. 5a, plotting $ln(mol(n)\%)$ vs. n, performing a linear regression analysis to find the gradient $ln\alpha$ and then exponentiating the result as a power of e [20].
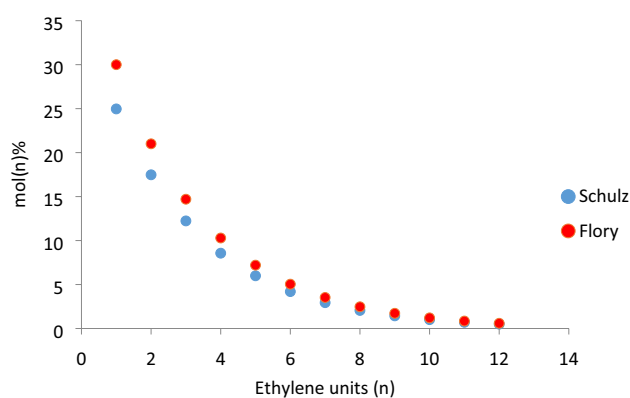

Fig. 4 Oligomer distribution in mol(n) % vs. n using Eqs. 1b (Schulz) and 3b (Flory) ($\alpha = 0.70$)

The value for α determined in this way will be the same in both cases.

By comparing Eq. 2c with Eq. 4b, it may be seen that:

$$wt(n)\% = c'n\alpha^n \tag{5b}$$

with $(ln\alpha)^2$ as the proportionality constant for Schulz and $(1 - \alpha)^2/\alpha$ as the proportionality constant for Flory (Table 1).

In the next section, a new derivation for Eq. 3a will be presented which utilises *recurrence relations*, followed by the presentation of a new back-solving method to determine α and R. The analysis lays the groundwork for an analogous consideration of second-order oligomerisation processes.

2.1.1 Derivation of the Schulz–Flory Equation via Recurrence Relations

Catalytic oligomerisation systems which give Schulz–Flory LAO distributions propagate either via a Cossee chain growth mechanism or via a metallacyclic mechanism (Schemes 2 and 3). Both mechanisms may be generically represented by Scheme 4. Deuterium labelling studies have shown that many chromium systems operate via the metallacyclic pathway [21–23].

In Scheme 4:

- R is the total amount in mol of oligomers produced (from T_1 onwards) during the reaction time i.e. the rate at which intermediate species arrive at $M(C_2)_n$, in units of mol t^{-1}.
- α is the propagation probability from $M(C_2)_n$ to $M(C_2)_{n+1}$ etc.
  - So $(1 - \alpha)$ is the elimination probability from $M(C_2)_n$ etc.

Table 1 Comparison of Schulz's equations and Flory's equations

	Schulz	Flory	Schulz and Flory
Derivation approach	Continuous function approximation	Direct (i.e. no continuous function approximation)	–
$mol(n)\%$	$mol(n)\% = -(ln\alpha)\alpha^n$	$mol(n)\% = (1-\alpha)\alpha^{n-1}$	$mol(n)\% = c\alpha^n$ $c = -(ln\alpha)$ for Schulz $c = (1-\alpha)/\alpha$ for Flory
$wt(n)\%$	$wt(n)\% = (ln\alpha)^2 n\alpha^n$	$wt(n)\% = n(1-\alpha)^2\alpha^{n-1}$	$wt(n)\% = c'n\alpha^n$ $c' = (ln\alpha)^2$ for Schulz $c' = (1-\alpha)^2/\alpha$ for Flory

Scheme 2 Cossee-type chain growth mechanism for Schulz–Flory LAO distributions. Active species and monomer shown in black, eliminated products shown in blue
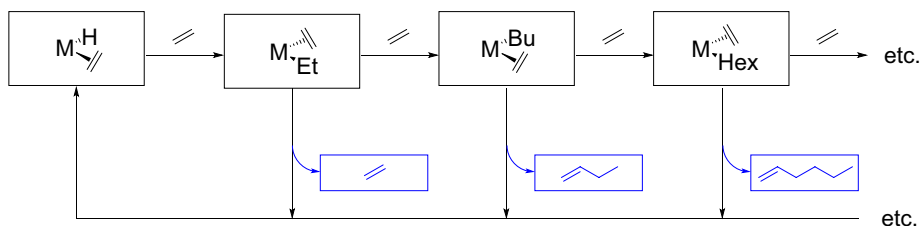
Scheme 3 Metallacyclic mechanism for Schulz–Flory LAO distributions. Active species and monomer shown in black, eliminated products shown in blue
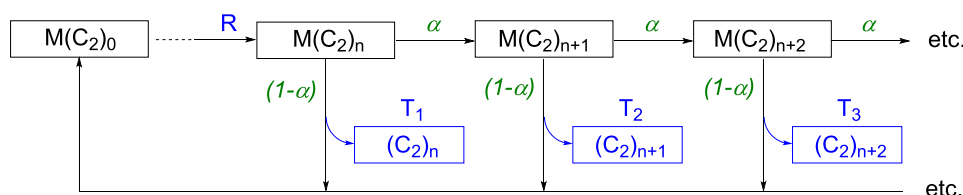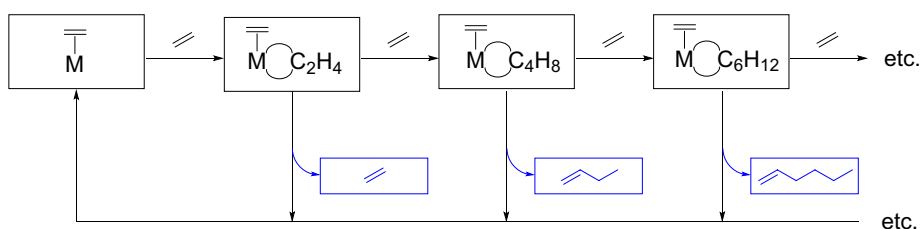
Scheme 4 Generic scheme for Schulz–Flory LAO distributions. Active species shown in black, rates and eliminated products shown in blue, probabilities of propagation and elimination pathways shown in green

- T_n is the total mol of a particular LAO with chain length $(C_2)_n$ produced during the reaction time (i.e. the rate at which that particular LAO is eliminated, in units of mol t^{-1}), with T_1 as the starting point in the sequence.

Expressions for each LAO fraction may be found by inspection of Scheme 4, or by using a recurrence relation methodology. These two techniques are demonstrated in the centre and right columns of Table 2 respectively.

The aim is to express T_n in terms of α and R. From inspection of the central column of Table 2, it may be inferred that the expression is:

Table 2 Expressions for T_n via inspection (centre) or via recurrence relation (right)

Term	Via inspection [18, 19]	Via recurrence relation [16]
T_1	$\underbrace{(1-\alpha)}_{\substack{\text{Probability of}\\\text{elimination}}}\underbrace{R}_{\substack{\text{Rate at which}\\\text{species arrive}}}$	T_1
T_2	$(1-\alpha)\alpha R$	αT_1
T_3	$(1-\alpha)\alpha^2 R$	αT_2
…	…	…
T_{n+1}	$(1-\alpha)\alpha^n R$	αT_n

$$T_{n+1} = (1-\alpha)\alpha^n R \leftrightarrow T_n = (1-\alpha)\alpha^{n-1}R \leftrightarrow mol(n) = (1-\alpha)\alpha^{n-1}R \tag{6}$$

Equation 6 is exactly the unnormalised Schulz–Flory equation, as per Eq. 3a.

Via the recurrence relation method, the general expression is:

$$T_{n+1} = \alpha T_n \leftrightarrow T_{n+1} - \alpha T_n = 0 \tag{7}$$

Following a derivation (see SI.1.4), the general solution for this expression is:

$$T_n = mol(n) = \frac{(1-\alpha)}{\alpha}R\alpha^n = (1-\alpha)\alpha^{n-1}R \tag{8}$$

i.e. the unnormalised Schulz–Flory equation, as per Eqs. 3a and 6.

With constant values for α and R, it is implicitly assumed that:

- The sequence begins at a suitable T_1 (e.g. a longer 1-alkene).
- The oligomerisation proceeds under steady state conditions (i.e. negligible change in ethylene pressure, reaction temperature and quantity of catalytic species).
  - Under steady state conditions, the standing quantities of each catalytic species are constant. The sum of rates to any particular active species "box" in Scheme 4 are equal to the sum of rates from that "box". This is equivalent to saying that the sum of probabilities for any particular active species "box" is 1 e.g. for $\boxed{M(C_2)_n}$ $R = \alpha R + (1-\alpha)R \leftrightarrow 1 = \alpha + (1-\alpha)$, for $\boxed{M(C_2)_{n+1}}$ $\alpha R = \alpha^2 R + \alpha(1-\alpha)R \leftrightarrow 1 = \alpha + (1-\alpha)$ etc.

2.1.2 Back-Solving to Determine α and R, and Checking for the Best Fit

In practice, the T_n terms are known (i.e. the amount in mol of each oligomer produced during the reaction time), and the aim is to find α and R. See SI.1.5 for a discussion on the method used to determine α and R, as well as a checking method to determine that the best fit has been found.

2.1.3 Application of the Fitting Procedure to Experiment

Bis(benzimidazole)pyridine chromium(III) chloride, in combination with MAO co-catalyst, gives a Schulz–Flory distribution of LAOs via a metallacyclic mechanism (Fig. 5) [24]. Fitting α either via a $ln(mol(n)\%)$ vs. n plot or via the recurrence relation method gives a resulting value of $\alpha = 0.84$.
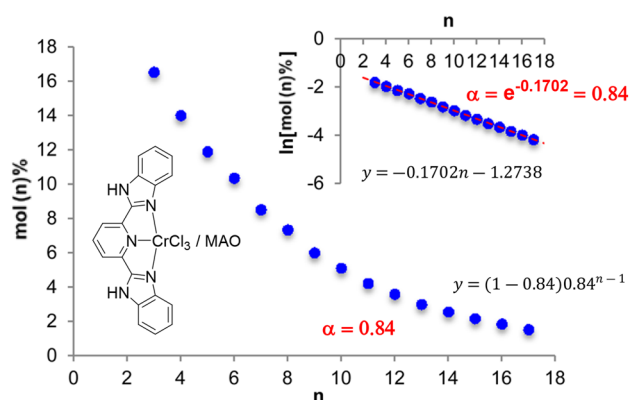
Fig. 5 Schulz–Flory LAO distribution as mol(n) % vs n (units of ethylene) obtained with bis(benzimidazole)pyridine chromium(III) chloride (1 µmol) [16, 24]. Inset: $ln(mol(n)\%)$ vs. n plot. Conditions: 4 bar of ethylene pressure, 30 °C, MAO (8 mmol), toluene (220 mL), 70 min. Activity = 5314 g mmol^{-1} h^{-1} bar^{-1}

It is worth noting that the determination of α via the recurrence relation method offers a subtle advantage over $ln(mol(n)\%)$ vs. n plots, in that accurate fits can *only* be obtained for distributions with reasonably constant α values as per Scheme 4. Linear regression analysis via the $ln(mol(n)\%)$ vs. n method may permit adequate fits for data sets displaying non-constant α behaviour, leading to Schulz–Flory equations which deviate from experimental plots.

2.1.4 Derivations of Further Experimentally-Relevant Metrics

For polymer distributions, M_n, M_w, and *PDI* are defined as follows:

$$M_n = \frac{\sum_{n=1}^{n=\infty} wt(n)}{\sum_{n=1}^{n=\infty} mol(n)} \tag{9a}$$

$$M_w = \sum_{n=1}^{n=\infty} wt(n)\% n \left(RFM\,C_2H_4\right) \tag{9b}$$

$$PDI = \frac{M_w}{M_n} \tag{9c}$$

These definitions can be applied to Schulz–Flory distributions. Using Eq. 3a, 4a and 4b the following expressions are obtained (see SI.1.6 for derivations):

$$M_n = \frac{\left(RFM\,C_2H_4\right)}{(1-\alpha)} \tag{9d}$$

$$M_w = \frac{(RFMC_2H_4)(1 + \alpha)}{(1 - \alpha)} \tag{9e}$$

$$PDI = (1 + \alpha) \tag{9f}$$

Note that α values are between 0 and 1. Consequently, *PDI* values are between 1 and 2 for Schulz–Flory distributions.

2.2 Second-Order Oligomerisation Processes

In 2006, Tomov et al. discovered a highly active chromium-based oligomerisation system, with activities in excess of 100,000 g mmol^{-1} h^{-1} bar^{-1}, which gave an alternating distribution of 1-alkenes via a metallacyclic mechanism (Fig. 6) [15].

The shape of this distribution cannot be described by first-order linear homogeneous recurrence relations with constant coefficients e.g. the Schulz–Flory equation. Variations on the first-order theme with orderly coefficients are likewise unable to accurately describe the experimentally-observed results. For instance, in a hypothetical alternating coefficients case, the quantities of the series of oligomers 1-hexene, 1-decene, 1-tetradecene etc. always decrease with *n*. Yet the distribution in Fig. 6 evidently displays some sort of periodicity.
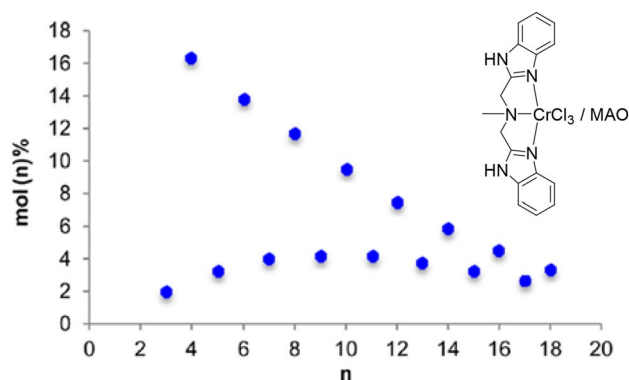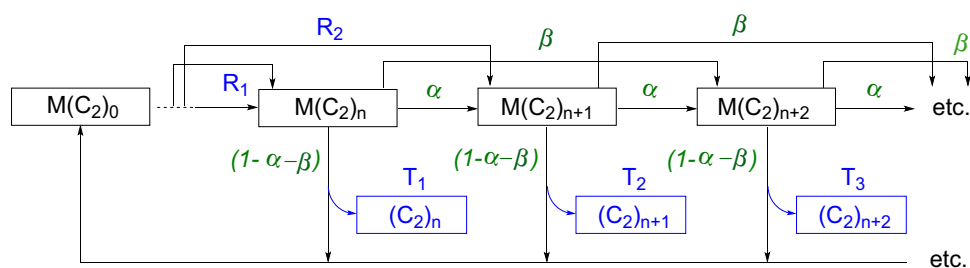

Fig. 6 Distribution of 1-alkene oligomers as mol(n)% vs n (units of ethylene) produced via *N,N*-bis((1H-benzimidazol-2-yl)methyl)-*N*-methylamine chromium(III) chloride/MAO [16, 17]. Conditions: 32 nmol Cr, 4 bar continuous ethylene pressure, 50 °C, MAO (7 mmol), toluene (200 mL), 1 h. Activity = 102,300 g mmol^{-1} h^{-1} bar^{-1}

All oligomerisations may be mathematically considered in terms of recurrence relations, so from an analytic point of view it is logical to proceed from a first-order treatment to a second-order treatment. Chemically speaking, this implies a mechanism involving both single and double coordination and insertion of ethylene. The double coordination and insertion of olefins has been proposed previously. Ystenes proposed a "trigger" mechanism whereby a coordinated olefin only inserts once a second olefin has coordinated to the metal [25]. Lemos and co-workers proposed a related mechanism based on kinetic studies of Ziegler–Natta catalysts [26], and a similar mechanism has been implicated in other oligomerisation processes [27, 28].

Building on the analysis from Sect. 2.1, a new "alternating equation" is derived here, which may be viewed as a direct analogue to the Schulz–Flory equation for second-order oligomerisation processes and which accurately describes alternating distributions as per Fig. 6. This is followed by the presentation of a new back-solving method for the determination of key mechanistic parameters.

2.2.1 Derivation of the Alternating Equation via Recurrence Relations

In Scheme 5:

- R_1 is the rate at which intermediate species arrive at $M(C_2)_n$, in units of mol t^{-1}.
- R_2 is the rate at which intermediate species originating from before $M(C_2)_n$ arrive at $M(C_2)_{n+1}$, in units of mol t^{-1}.
  - So the total amount in mol of oligomers, R, produced (from T_1 onwards) during the reaction time is expressed by $R = R_1 + R_2$
- α is the propagation probability from $M(C_2)_n$ to $M(C_2)_{n+1}$ etc.
- β is the propagation probability from $M(C_2)_n$ to $M(C_2)_{n+2}$ etc.
  - So $(1 - \alpha - \beta)$ is the probability of elimination from $M(C_2)_n$ etc.
- T_n is the total mol of a particular 1-alkene with chain length $(C_2)_n$ produced during the reaction time (i.e. the

Scheme 5 Catalytic scheme for the production of alternating 1-alkene oligomer distributions. Active species shown in black, rates and eliminated products shown in blue, probabilities of propagation and elimination pathways shown in green

Table 3 Expressions for T_n via inspection (centre) or via recurrence relation (right)

Term	Via inspection	Via recurrence relation [16]
T_1	$\underbrace{(1 - \alpha - \beta)}_{\substack{\text{Probability of} \\ \text{elimination}}}\underbrace{R_1}_{\substack{\text{Rate at which} \\ \text{species arrive}}}$	T_1
T_2	$(1 - \alpha - \beta)(\alpha R_1 + R_2)$	$\alpha T_1 + T_1'$
T_3	$(1 - \alpha - \beta)\left[\alpha(\alpha R_1 + R_2) + \beta R_1\right]$	$\alpha T_2 + \beta T_1$
…	…	…
T_{n+2}	–	$\alpha T_{n+1} + \beta T_n$

rate at which that particular 1-alkene is eliminated, in units of mol t^{-1}), with T_1 as the starting point in the sequence.

With reference to Scheme 5, Table 3 expresses each LAO via inspection (central column) or via recurrence relation (right column). The aim is to express T_n in terms of α, β, R_1 and R_2. In contrast to Sect. 2.1, obtaining a general expression via inspection is no longer feasible. The method of solving via a recurrence relation is much more straightforward, as will be demonstrated below.

The recurrence relation is:

$$T_{n+2} = \alpha T_{n+1} + \beta T_n \leftrightarrow T_{n+2} - \alpha T_{n+1} - \beta T_n = 0 \quad (10)$$

Following a derivation (see SI.2.1), the general solution to this expression is: [16]

$$T_n = mol(n) = c_1 r_1^n + c_2 r_2^n$$

with:

$$r_1 = \frac{\alpha + \sqrt{\alpha^2 + 4\beta}}{2}$$

$$r_2 = \frac{\alpha - \sqrt{\alpha^2 + 4\beta}}{2}$$

$$c_1 = \frac{(1 - \alpha - \beta)(R_1 r_1 + R_2)}{r_1(r_1 - r_2)}$$

$$c_2 = \frac{(1 - \alpha - \beta)(R_1 r_2 + R_2)}{r_2(r_2 - r_1)} \quad (11)$$

i.e. the unnormalised alternating equation.

With constant values for α, β, R_1 and R_2, it is implicitly assumed that:

- The sequence begins at a suitable T_1 (e.g. a longer 1-alkene)
- The oligomerisation proceeds under steady state conditions (i.e. negligible change in ethylene pressure, reaction temperature and quantity of catalytic species)
- Under steady state conditions, the standing quantities of each catalytic species are constant. The sum of rates to any particular active species "box" are equal the sum of rates from that "box". This is equivalent to saying that the sum of probabilities from any particular active species "box" is 1 e.g. for $\boxed{M(C_2)_n}$ $R_1 = \alpha R_1 + \beta R_1 + (1 - \alpha - \beta)R_1 \leftrightarrow 1 = \alpha + \beta + (1 - \alpha - \beta)$ for $\boxed{M(C_2)_{n+1}}$ $\alpha R_1 + R_2 = \alpha(\alpha R_1 + R_2) + \beta(\alpha R_1 + R_2)$ $+(1 - \alpha - \beta)(\alpha R_1 + R_2) \leftrightarrow \alpha R_1 = \alpha^2 R_1 + \beta \alpha R_1 + (1 - \alpha - \beta)\alpha R_1 \leftrightarrow 1 = \alpha + \beta + (1 - \alpha - \beta)$, etc.

To convert the unnormalised alternating equation, Eq. 11, into the normalised form:

$$mol(n)\% = \frac{mol(n)}{\sum_{n=1}^{n=\infty} mol(n)} = \frac{c_1 r_1^n + c_2 r_2^n}{R_1 + R_2} \quad (12)$$

or equivalently (see SI.2.2):

$$mol(n)\% = \frac{c_1 r_1^n + c_2 r_2^n}{\frac{c_1 r_1}{1 - r_1} + \frac{c_2 r_2}{1 - r_2}} \quad (13)$$

Converting Eq. 11 into an unnormalised $wt(n)$ equivalent:

$$wt(n) = n(RFMC_2H_4)mol(n) = n(RFMC_2H_4)(c_1 r_1^n + c_2 r_2^n) \quad (14)$$

which gives (see SI.2.3):

$$wt(n)\% = \frac{n(c_1 r_1^n + c_2 r_2^n)}{\frac{c_1 r_1}{(1 - r_1)^2} + \frac{c_2 r_2}{(1 - r_2)^2}} \quad (15)$$

2.2.2 Back-Solving to Determine α, β, R_1, and R_2, and Checking for the Best Fit

In practice, the T_n terms are known (i.e. the amount in mol of each oligomer produced during the reaction time), and the aim is to find α, β, R_1, and R_2. See SI.2.4 for a discussion on the method used to determine α and R, as well as a checking method to determine that the best fit has been found.

2.2.3 Application of the Fitting Procedure to Experiment

See Sect. 2.4 for examples of fittings using the described recurrence relation method with

N,N-bis((1H-benzimidazol-2-yl)methyl)-N-methylamine chromium(III) chloride/MMAO-12 systems.

2.2.4 Derivations of Further Experimentally-Relevant Metrics

As per Schulz–Flory distributions, the definitions of M_n, M_w and PDI in Eqs. 9a, 9b, 9c can be applied to alternating distributions. Using Eqs. 11, 14 and 15, and Eqs. 12ii and 14iii in SI, the following expressions are obtained (see SI.2.5 for derivations):

$$M_n = \frac{\left(RFMC_2H_4\right)}{\frac{c_1 r_1}{1-r_1} + \frac{c_2 r_2}{1-r_2}} \left[\frac{c_1 r_1}{\left(1-r_1\right)^2} + \frac{c_2 r_2}{\left(1-r_2\right)^2} \right] \quad (16a)$$

$$M_w = \frac{\left(RFMC_2H_4\right)}{\frac{c_1 r_1}{(1-r_1)^2} + \frac{c_2 r_2}{(1-r_2)^2}} \left[\frac{c_1 r_1\left(1+r_1\right)}{\left(1-r_1\right)^3} + \frac{c_2 r_2\left(1+r_2\right)}{\left(1-r_2\right)^3} \right] \quad (16b)$$

$$PDI = \frac{py + qx}{\left[py^2 + qx^2\right]^2} \left[py^3(2-x) + qx^3(2-y) \right]$$

with:

$$p = c_1 r_1$$

$$q = c_2 r_2$$

$$x = 1 - r_1$$

$$y = 1 - r_2 \quad (16c)$$

Note that with $q = 0$, $y = 1$, and $r_1 = \alpha$, PDI matches the expression previously obtained with Schulz–Flory distributions (see Eq. 9f):

$$PDI = \frac{p}{p^2} p(2-x) = 2 - x = 1 + r_1 = 1 + \alpha$$

As with Schulz–Flory distributions, PDI values for alternating distributions lie between 1 and 2. This may be demonstrated by examining four limiting cases (see SI.2.6).

2.3 Connecting First-Order and Second-Order Oligomerisation Processes

By inspection of Eq. 11, two cases may be identified where the second-order general solution collapses to a first-order solution as per Eq. 10. In the first case, if $\beta = 0$, then from Eq. 10iv $r_1 = \alpha$ and from Eq. 10v $r_2 = 0$. With $r_2 = 0$, Eq. 10xiii gives $R_2 = 0$. Then, using Eqs. 10x and 10xi (in SI.2.1 and SI.2.4):

$$c_1 r_1^n = \frac{(1-\alpha)R_1 r_1}{r_1\left(r_1 - r_2\right)} r_1^n = \frac{(1-\alpha)}{\left(r_1 - r_2\right)} r_1^n R_1$$
$$= \frac{(1-\alpha)}{(\alpha - 0)} \alpha^n R_1 = (1-\alpha)\alpha^{n-1} R_1 \quad (17a)$$

$$c_2 r_2^n = \frac{(1-\alpha)R_1 r_2}{r_2\left(r_2 - r_1\right)} r_2^n = \frac{(1-\alpha)}{\left(r_2 - r_1\right)} r_2^n R_1 = \frac{(1-\alpha)}{(0-\alpha)} 0^n R_1 = 0 \quad (17b)$$

Since $R_2 = 0$, then $R_1 = R$. Using Eq. 11, the general solution is therefore:

$$T_n = (1-\alpha)\alpha^{n-1} R \quad (18)$$

i.e. the unnormalised Schulz–Flory equation.

In the second, more general case, if $c_2 = 0$ but β is not necessarily 0, then with Eqs. 10xii and 10xiii in Supplementary Information (SI.2.4):

$$R_1 = \frac{r_1 c_1}{(1-\alpha-\beta)}$$

$$R_2 = \frac{-r_1 r_2 c_1}{(1-\alpha-\beta)}$$

$$\to R_2 = -r_2 R_1 \leftrightarrow \frac{R_2}{R_1} = -r_2 \quad (19)$$

Using Eq. 10v (Supplementary Information SI.2.1), Eq. 19 becomes:

$$\frac{R_2}{R_1} = \frac{-\alpha + \sqrt{\alpha^2 + 4\beta}}{2} \quad (20)$$

Using Eq. 19 with Eqs. 10x and 10xi (in SI.2.1):

$$c_1 r_1^n = \frac{(1-\alpha-\beta)\left(R_1 r_1 - R_1 r_2\right)}{r_1\left(r_1 - r_2\right)} r_1^n = \frac{(1-\alpha-\beta)\left(r_1 - r_2\right)}{\left(r_1 - r_2\right)}$$
$$r_1^{n-1} R_1 = (1-\alpha-\beta) r_1^{n-1} R_1 \quad (21a)$$

$$c_2 r_2^n = \frac{(1-\alpha-\beta)\left(R_1 r_2 - R_1 r_2\right)}{r_2\left(r_2 - r_1\right)} r_2^n = \frac{(1-\alpha-\beta)\left(r_2 - r_2\right)}{\left(r_2 - r_1\right)}$$
$$r_2^{n-1} R_1 = \frac{(1-\alpha-\beta)0}{\left(r_2 - r_1\right)} r_2^{n-1} R_1 = 0 \quad (21b)$$

From Eq. 11, the general solution is therefore:

$$T_n = (1-\alpha-\beta) r_1^{n-1} R_1 \quad (22)$$

which gives the unnormalised Schulz–Flory equation if $\beta = 0$. The second case may be summarised by stating that given particular values for α and β, R_2/R_1 may be tuned to generate first-order behaviour.

In this sub-section, the mathematics of the second case is illustrated, followed by a method to describe the degree of similarity between second-order recurrence relations and first-order ones. This analysis has important implications for the fitting of more "gently" alternating oligomer distributions.

2.3.1 The First-Order Surface in R_2/R_1, α and β Space

Equation 20 features three variables, R_2/R_1, α and β, which are physically interpretable as per Scheme 5. Conveniently, then, it is possible to plot in 3D space the combinations of R_2/R_1, α and β values which give rise to first-order behaviour. Furthermore, since r_2 does not feature in Eq. 22 and since β is not necessarily 0, Eq. 10iv (Supplementary Information SI.2.1) now operates as a parametric equation where different combinations of α and β may give the same result for r_1. A visualisation of the first-order surface in R_2/R_1, α and β space, constructed by lines along which r_1 is constant, is shown in Fig. 7 and 8. Note that first-order distributions following Eq. 18 are restricted to the alpha axis with $\beta = 0$ and $R_2/R_1 = 0$.

2.3.2 Degree of Alternation

By sight, it is evident that second-order distributions can possess varying degrees of alternating character. To arrive at a definition for the degree of alternation in a second-order distribution, we need to consider the pictorial representation of Eq. 11.

Figure 9 illustrates how an alternating distribution is mathematically constructed by adding a constantly decreasing first-order recurrence relation to an alternating first-order recurrence relation (recall that with $0 \le \alpha < 1$, $0 \le \beta < 1$, and $0 < (1 - \alpha - \beta) < 1$, then $0 < r_1 < 1$, $-1 < r_2 < 0$, and also $|r_2| \le |r_1|$). The degree of alternation is defined as:

$$Deg.\, of\, Alt. = \frac{\sum_{n=1}^{n=\infty} |c_2||r_2|^n}{\sum_{n=1}^{n=\infty} c_1 r_1^n} = \frac{|c_2|}{c_1} \frac{\sum_{n=1}^{n=\infty} (-r_2)^n}{\sum_{n=1}^{n=\infty} r_1^n} \quad (23a)$$

Absolute values are taken in the numerator to avoid cancellation of terms on summation (refer to Fig. 9). $0 < c_1$ (see Eq. 10viii in Supplementary Information SI.2.1) so $0 < \sum_{n=1}^{n=\infty} c_1 r_1^n$. Given that $-1 < r_2 < 0$, then $|r_2|^n = (-r_2)^n$.

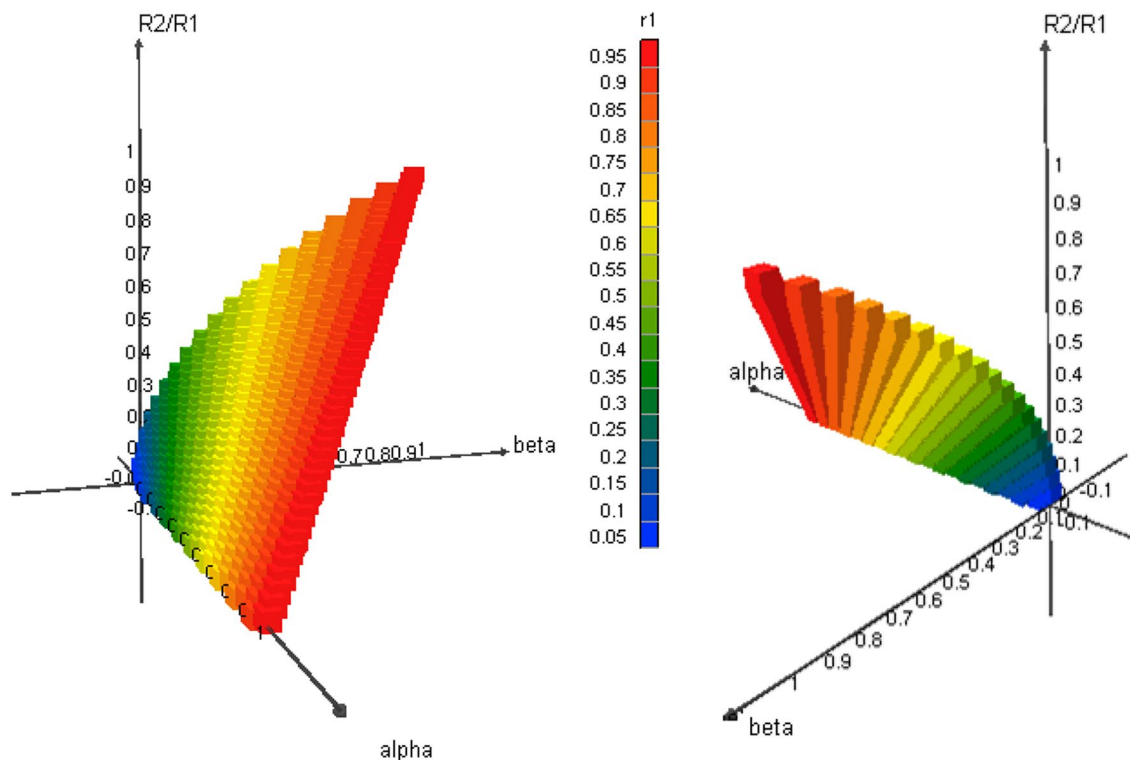Evaluation of Eq. 23a (in SI.3.1) gives the following result:

Fig. 7 Visualisation of the first-order surface in R_2/R_1, α and β space along the α axis (left) and along the β axis (right). Colours correspond to particular values of r_1 (key centre)
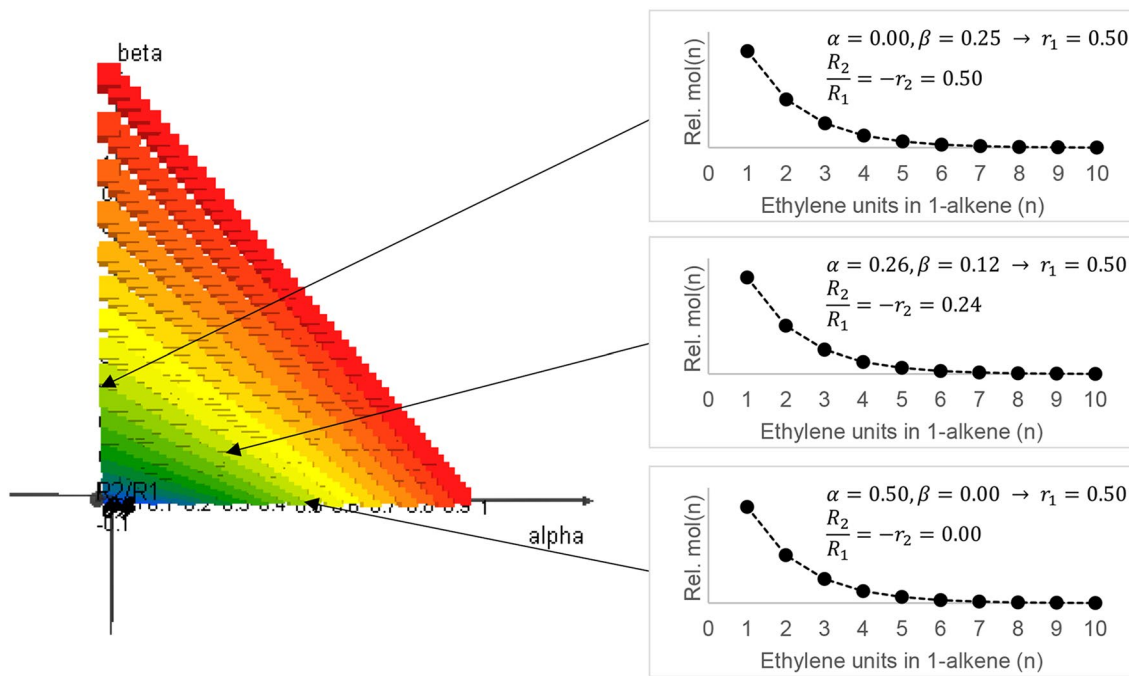
Fig. 8 Visualisation of the first-order surface in R_2/R_1, α and β space along the R_2/R_1 axis. Optically identical first-order distributions with $r_1 = 0.50$ illustrated

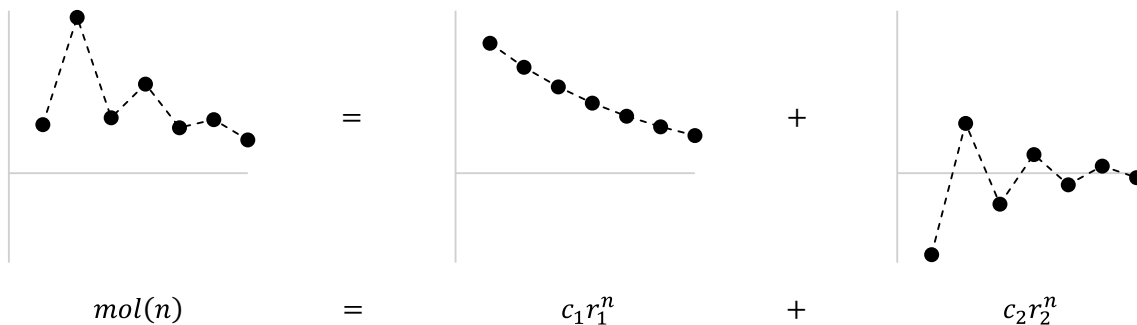$$mol(n) \qquad = \qquad c_1 r_1^n \qquad + \qquad c_2 r_2^n$$

Fig. 9 Pictorial representation of Eq. 11

$$Deg.\ of\ Alt. = \frac{+\sqrt{\left(r_2 + \frac{R_2}{R_1}\right)^2 (1 - r_1)}}{\left(r_1 + \frac{R_2}{R_1}\right)(1 + r_2)} \qquad (23b)$$

Since $0 < r_1 < 1$, $-1 < r_2 < 0$, and $|r_2| \leq |r_1|$, then $0 \leq Deg.\ of\ Alt. < 1$ (i.e. $Deg.\ of\ Alt.$ may be considered as a percentage).

As r_1 and r_2 may be expressed in terms of α and β, Eq. 23b gives the degree of alternation as a function of $R_2/R_1, \alpha$ and β. In other words, every point in $R_2/R_1, \alpha$ and β space has an associated degree of alternation. A visualisation of the degree of alternation map in $R_2/R_1, \alpha$ and β

space is shown in Fig. 10. Note that although $0 \leq R_2/R_1$, for convenience Fig. 10 runs only from $0 \leq \frac{R_2}{R_1} \leq 1$.

The red areas in Fig. 10 represent those areas with the largest degree of alternation, i.e. where R_2/R_1 or β are highest. The light blue layer corresponds to the first-order surface shown in Figs. 7 and 8, where distributions display no degree of alternation. This layer acts as a crossing-point, above which distributions display "normal" alternating behaviour, and below which distributions display "inverse" alternation. Figure 11 illustrates these results. Note that in Fig. 11, α and β remain constant while R_2/R_1 varies. While experimentally so far only "normal" alternating distributions
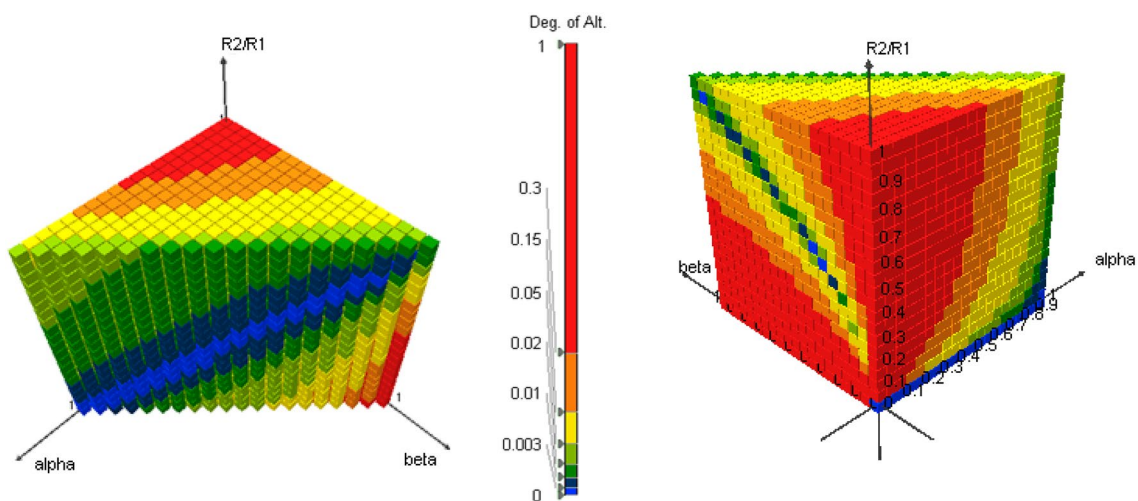
Fig. 10 Front (left) and back (right) view of the degree of alternation map in R_2/R_1, α and β space. Colours correspond to particular values for degree of alternation (key centre)

$\alpha = 0.20, \beta = 0.50, \dfrac{R_2}{R_1} = 5.000$

$T_n = (0.50)(0.814)^n + (0.50)(-0.614)^n$

$Deg. \, of \, Alt. = 0.36$

$\alpha = 0.20, \beta = 0.50, \dfrac{R_2}{R_1} = 0.614$

$T_n = (0.50)(0.814)^n + (0.00)(-0.614)^n$

$Deg. \, of \, Alt. = 0.00$

$\alpha = 0.20, \beta = 0.50, \dfrac{R_2}{R_1} = 0.000$

$T_n = (0.50)(0.814)^n + (-0.50)(-0.614)^n$
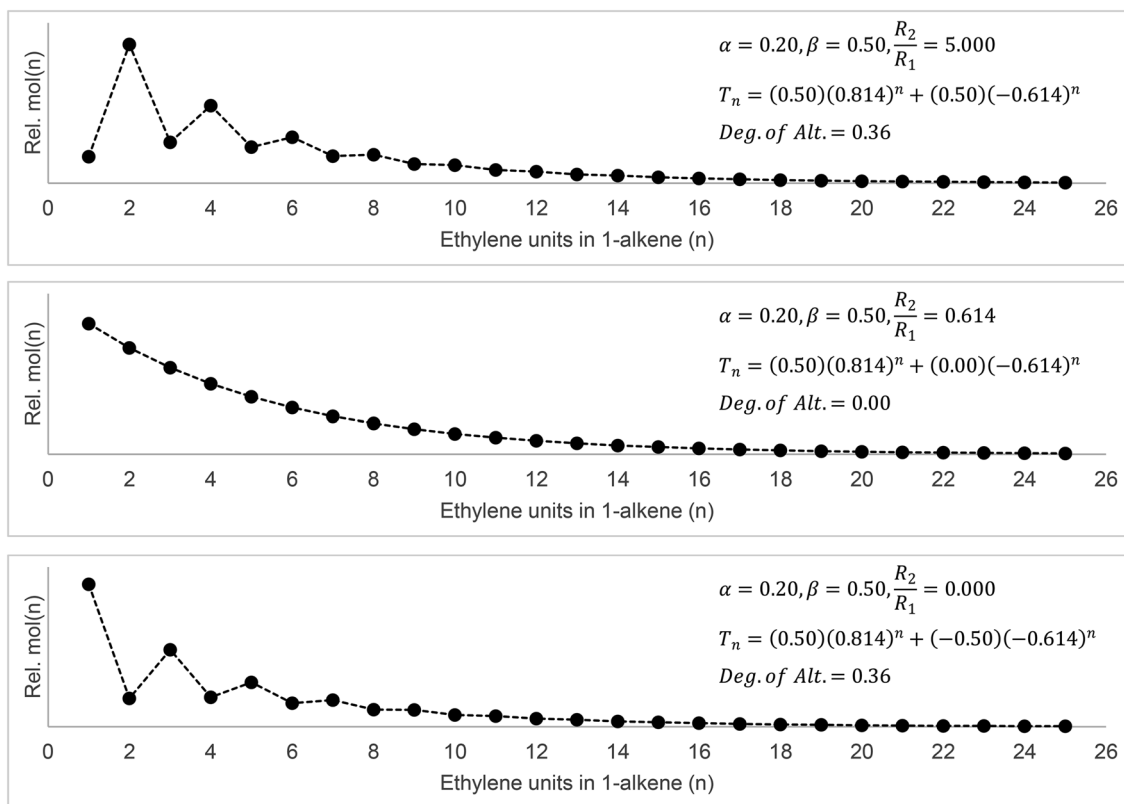
$Deg. \, of \, Alt. = 0.36$

Fig. 11 Examples of distributions obtained above the first-order surface (top) showing "normal" alternating behaviour, on the first-order surface (middle), and below the first-order surface (bottom) showing "inverse" alternating behaviour

have been found, the discovery of "inverse" alternating behaviour is theoretically possible.

2.3.3 Implications for Second-Order Fitting with "Gently" Alternating Distributions

"Gently" alternating distributions display significantly less $c_2 r_2^n$ character than $c_1 r_1^n$ character. Such distributions lie close to the first-order surface in R_2/R_1, α and β space as illustrated in Figs. 7 and 8. In back-solving to determine α, β, R_1, and R_2, "gently" alternating distributions present a unique difficulty in the fitting process when experimental error is taken into account.

The first-order surface in Figs. 7 and 8 is constructed by lines along which r_1 is constant and along which distributions appear identical. Second-order distributions which are similar in appearance, but which lie close to the first-order surface, may accurately be described using quite different R_2/R_1, α and β values.

By way of illustration, consider the hypothetical second-order distribution shown in Fig. 12, as may be detected via GC from 1-hexene onward. If, due to experimental error, a quantity of 1-hexene evaporates prior to GC measurement, then the back-solving method produces a different fit for the data set slightly perturbed at C_6.

Comparing the fitted parameters in Fig. 12 with those in Fig. 13, there are significant differences between values for α, β, R_2/R_1, c_2 and r_2. The only reliable metric for "gently" alternating distributions is the first-order $c_1 r_1^n$ term. In borderline cases where a second-order distribution lies too close to the first-order surface to obtain reliable values for α,

β, R_1, and R_2, pressure studies (see Sect. 2.4) and/or repeat experiments will be necessary.

2.4 The Effect of Pressure in Second-Order Steady-State Oligomerisation

In Sect. 2.2, a catalytic scheme (Scheme 5) for the production of alternating 1-alkene oligomer distributions was presented. The terms $M(C_2)_n$, $M(C_2)_{n+1}$ etc. group together all intermediates involving n ethylene units. In order to investigate the effect of changing ethylene pressure on α and β, it is necessary to propose a more detailed scheme with the individual elementary reaction steps that occur within each active species "box" (i.e. between each type of $M(C_2)_n$ species). This so-called candidate scheme is kept as general as possible, for application to any processes proceeding via a metallacyclic mechanism (Scheme 6):

Following a derivation (see SI.4.1), it can be shown that the ratio between the probabilities for double ethylene insertion β and single insertion α is defined as:

$$\frac{p(2Et\,inserted)}{p(1Et\,inserted)} = \frac{\frac{k_2 k_7 P_{et}}{k_H}}{k_5(k_3 + k_6 + k_7 + k_{10}) + \frac{k_2 k_6 P_{et}}{k_H}} \quad (24a)$$

So long as $k_2, k_7 \neq 0$, the relationship between the probabilities α and β and ethylene pressure P_{et} can be expressed as:

$$\frac{\beta}{\alpha} = \frac{P_{et}}{g_1 + g_2 P_{et}} \quad (24b)$$

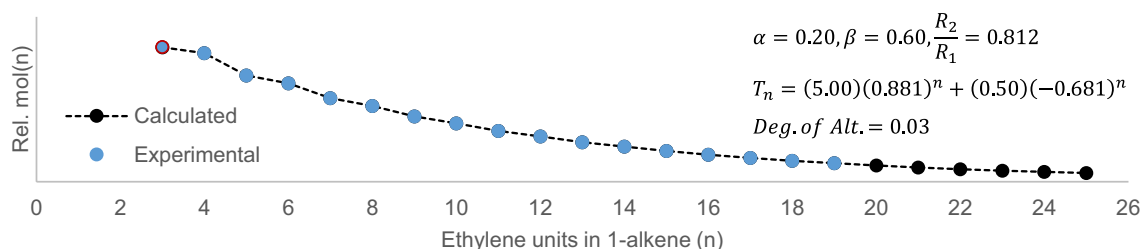$$\alpha = 0.20, \beta = 0.60, \frac{R_2}{R_1} = 0.812$$

$$T_n = (5.00)(0.881)^n + (0.50)(-0.681)^n$$

$$Deg.\,of\,Alt. = 0.03$$

Fig. 12 Hypothetical second-order "gently" alternating distribution

$$\alpha = 0.38, \beta = 0.44, \frac{R_2}{R_1} = 0.985$$

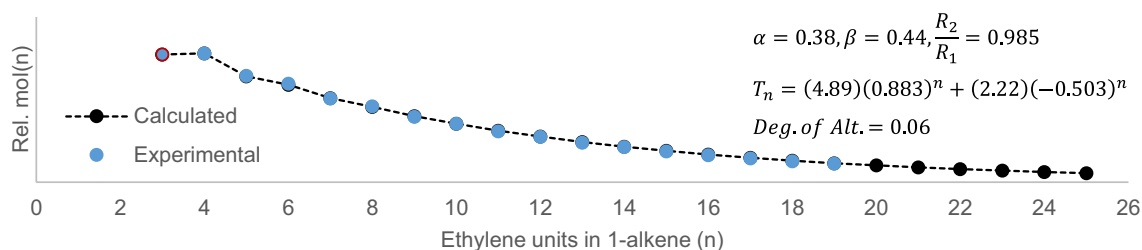$$T_n = (4.89)(0.883)^n + (2.22)(-0.503)^n$$

$$Deg.\,of\,Alt. = 0.06$$

Fig. 13 Hypothetical second-order "gently" alternating distribution with some 1-hexene missing

where:

$$g_1 = \frac{k_5(k_3 + k_6 + k_7 + k_{10})k_H}{k_2 k_7} = \text{a constant across} P_{et}$$

$$g_2 = \frac{k_6}{k_7} = \text{a constant across} P_{et}$$

Scheme 6 Candidate scheme proposed for individual reaction steps occurring between each type of metallacyclic $M(C_2)_n$ species, with selected rate constants labelled
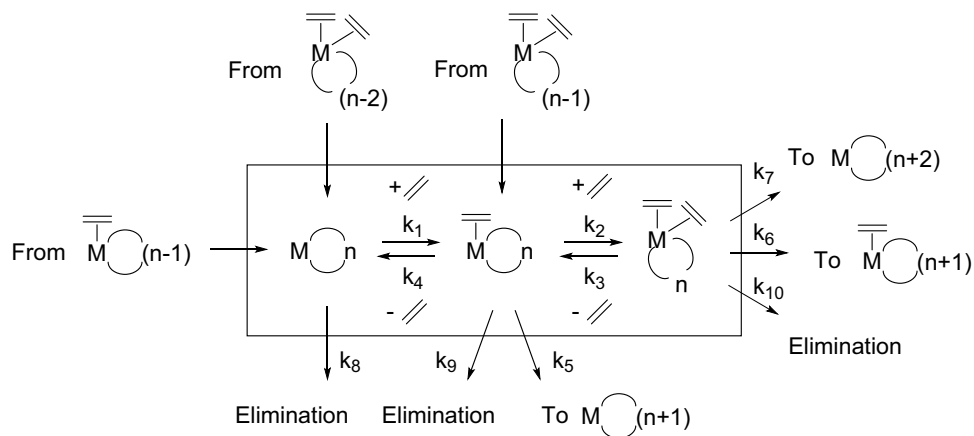

Table 4 Key parameters in the fitting of second-order oligomerisation parameters vs. ethylene pressure

Pressure/barg[b]	Olig/g[c]	mol(n) %[d]	α	β	$1-\alpha-\beta$	β/α	c_2/c_1	Deg. of Alt.	R^2 fit[e]
0.3	0.04	Tn = (0.26)*(0.874)^n + (0.15)*(−0.443)^n	0.43	0.39	0.18	0.90	0.56	0.06	0.997
0.5	0.10	Tn = (0.22)*(0.874)^n + (0.07)*(−0.611)^n	0.26	0.53	0.20	2.03	0.34	0.08	0.993
0.7	0.09	Tn = (0.24)*(0.854)^n + (0.10)*(−0.642)^n	0.21	0.55	0.24	2.59	0.43	0.13	0.996
1	0.35	Tn = (0.19)*(0.883)^n + (0.15)*(−0.674)^n	0.21	0.60	0.20	2.86	0.80	0.22	0.997
2	0.65	Tn = (0.18)*(0.883)^n + (0.15)*(−0.711)^n	0.17	0.63	0.20	3.64	0.82	0.27	0.996
3	1.52	Tn = (0.17)*(0.887)^n + (0.14)*(−0.734)^n	0.15	0.65	0.20	4.26	0.80	0.28	0.997
4	2.30	Tn = (0.18)*(0.883)^n + (0.15)*(−0.740)^n	0.14	0.65	0.20	4.57	0.87	0.33	0.996

[a]Conditions: 30 nmol Cr, continuous ethylene pressure, 50 °C, MMAO-12 (5 mmol), toluene (200 mL), 1 h
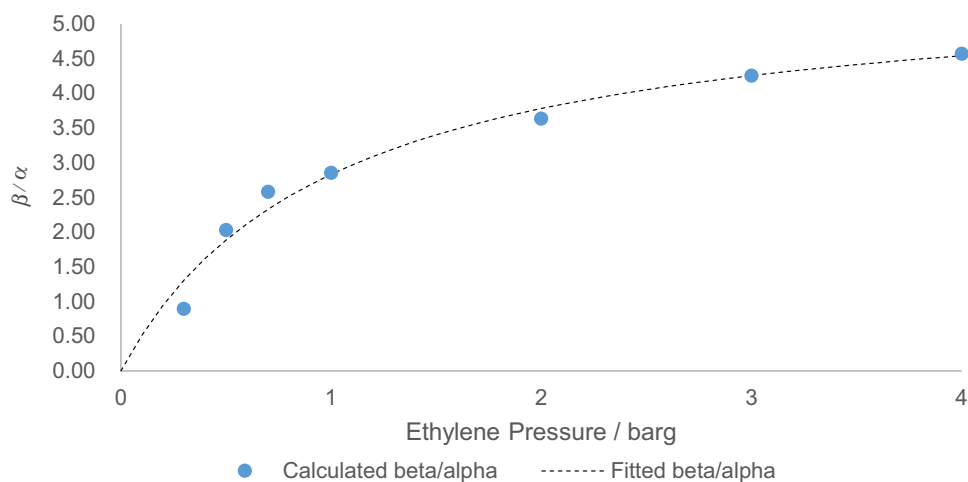
[b] x barg = 1 bar N_2 + x bar ethylene (barg = gauge pressure)

[c]n = 4 + oligomers

[d]Data from C_8 onwards, C_6 as T_1

[e]R^2 indicates the goodness of fit between experimental and calculated data sets

Fig. 14 Experimentally determined β/α values vs. pressure, together with fitted curve according to Eq. 24b

2.4.1 Comparison of Experimentally Determined Results vs. Fitted Data

A series of oligomerisation experiments have been performed at different ethylene pressures, using *N*,*N*-bis((1H-benzimidazol-2-yl)methyl)-*N*-methylamine chromium(III) chloride/MMAO-12 as the catalyst (experimental details as per ref. 17). The α and β values for each run were obtained using the back-solving method described in Sect. 2.2, and the values of β/α were plotted vs. ethylene pressure. A curve following Eq. 24b was fitted to these calculated values, using a minimisation of the sum of squared differences to determine the most suitable values for g_1 and g_2. The results are given in Table 4 and Fig. 14.

The fitting of the data in Table 4 with Eq. 24b gives values for $g_1 = 0.177$ and $g_2 = 0.176$. Note that g_2 is equivalent to the ratio of rate constants for single insertion vs. double insertion from a double-ethylene associated intermediate. There is a good degree of correlation between experimentally determined and the fitted values of β/α in Fig. 14 (goodness of fit $R^2 = 0.974$).

A final note should be added, that for ethylene oligomerisations at lower pressures with these catalysts, it is possible that the most abundant oligomeric product, 1-butene in this case, is incorporated during the oligomerisation reaction. We have observed this with some of the most active catalysts, resulting in a minor distribution of 2-ethyl-1-alkenes with the opposite alternating pattern, alongside the major distribution of 1-alkenes with the normal alternating behaviour [17].

2.5 Steady-State Oligomerisation with Nonconstant Propagation Probabilities

In assuming constant values for the propagation probabilities α and β in Schemes 4 and 5 (Sects. 2.1 and 2.2 respectively), recurrence relations with constant coefficients are generated.

The solution of these may be expressed in equation format (see Eqs. 8 and 11). If, however, the propagation probabilities adopt nonconstant values in the catalytic cycle, then recurrence relations with variable coefficients are generated. The aim in such cases is to determine a unique value for each unknown parameter, and/or to elucidate the key mechanistic features of the system.

In this sub-section, a method for handling first-order recurrence relations with variable coefficients is presented. The method finds application in oligomerisation systems where α changes at some point in the catalytic cycle. Second-order systems with nonconstant propagation probabilities will be discussed later, with a particular focus on selective-tetramerisation.

2.5.1 First-Order Recurrence Relations with Nonconstant Propagation Probabilities

Experimental LAO distributions which deviate from Schulz–Flory have been observed, for example chromium(III) bis(carbene)pyridine systems reported by McGuinness and co-workers (Fig. 15) [29]. The observation has been rationalised by less favourable elimination at the early stages of metallacyclic growth [29]. In Fig. 15, α is variable before C_8, then adopts a constant value from C_8 onwards.

Data from C_8 (n = 4) onward may be treated with the back-solving method described in Sect. 2.1 to find the constant α value and R, the total mol of C_{8+} oligomers produced during the reaction time (i.e. the rate at which intermediate species arrive at $\boxed{M(C_2)_4}$. Adapting Scheme 4 to show rates, the first nonconstant term T_1' (i.e. C_6) may be appended, along with R', the rate at which intermediate species arrive at $\boxed{M(C_2)_3}$ (Scheme 7).

To find α' (i.e. the α value at C_6) and R', two distinct equations involving the two unknown variables may be identified (note that T_1' is the experimental data point for 1-hexene):
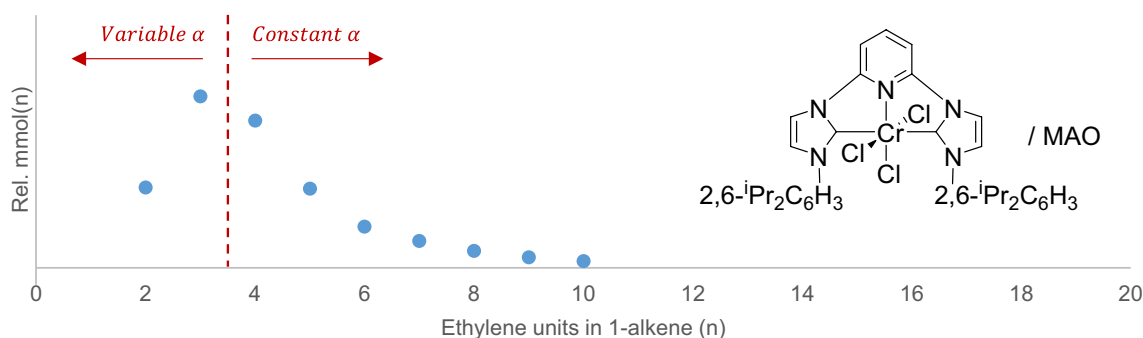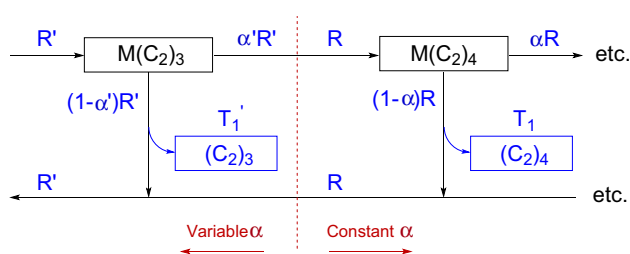

Fig. 15 Distribution of 1-alkene oligomers as relative mol(n) vs n (units of ethylene) produced with complex 2,6-bis(1-(2,6-diisopropylphenyl)imidazol-2-ylidene)pyridine chromium(III) chloride. Conditions: 10 µmol Cr, 5 bar continuous ethylene pressure, 25 °C, MAO (5 mmol), toluene (50 mL), 30 min. Activity (C_4–C_{20} LAOs) = 159 g mmol^{-1} h^{-1} bar^{-1}. Variable α and constant α regions indicated

Scheme 7 Catalytic scheme for Fig. 15 at the boundary of the variable α and constant α regions. Active species shown in black, rates and eliminated products shown in blue

$$\alpha' R' = R \tag{25a}$$

$$\left(1 - \alpha'\right)R' = T_1' \tag{25b}$$

These equations sum to give:

$$R' = T_1' + R \tag{25c}$$

Given that there are two distinct equations for two unknowns (α' and R'), a unique solution does exist. R' may be found with Eq. 25c, then substituted into Eqs. 25a or 25b to find α'. The second non-constant term T_2' (i.e. C_4) may now be appended to Scheme 7, and the α value at C_4 found using the same methodology. The α values calculated for Fig. 15 via this methodology are 0.86, 0.65 and 0.54 from C_4, C_6 and C_{8+} respectively. In other words, for this particular chromium catalyst, the termination probability is less favourable at the early stages and increases as the metallacycle grows from a metallacyclopentane to—heptane and—nonane. Once the metallacycle has reached a certain size, the termination probability becomes constant.

2.5.2 Second-Order Recurrence Relations with Nonconstant Propagation Probabilities

McGuinness, Britovsek and co-workers produced a detailed experimental and theoretical study of single- and double-coordination mechanisms in ethylene tri- and tetramerisation with Cr/PNP catalysts [30]. With PNP = $Ph_2PN(^iPr)$ PPh_2, high selectivity for 1-octene is observed (~ 70 mol%), together with approximately 16 mol% 1-hexene, 3 mol% C_{10+} α-olefins, and various other coproducts (Fig. 16).

Computational studies employing the M06L functional on simplified model compounds have indicated that a single- and double-coordination mechanism operates (see Fig. 17) [30–33]. Elimination from a chromacyclopentane intermediate to give 1-butene is calculated to be energetically unfavourable [30]. Competing processes to 1-hexene and 1-octene formation diverge at a singly-coordinated chromacyclopentane intermediate **7**, with 1-hexene formed predominately via single insertion

from intermediate **7**, and 1-octene formed predominantly via a bis(ethylene) metallacyclic intermediate **17**, with additional involvement of a mono(ethylene) route through intermediate **18** [30].

Given the varying differences in energy between the early intermediates in Fig. 17, the selective-tetramerisation process in Fig. 16 may be mathematically considered as a second-order recurrence relation with variable coefficients. Data from C_{16} onwards corresponds to the tail end of an alternating distribution, where α and β values are constant by virtue of negligible geometry and energy differences between larger chromacyclic species. For the purpose of the present discussion, setting aside the difficulties in fitting gently alternating distributions as outlined in Sect. 2.3, the region from C_{16} onwards may conceivably be treated with the back-solving method described in Sect. 2.2 to find the constant values for α and β as well as R_1, the rate at which intermediate species arrive at $\boxed{M(C_2)_8}$, and R_2, the rate at which intermediate species originating from before $\boxed{M(C_2)_8}$ arrive at $\boxed{M(C_2)_{10}}$. Adapting Scheme 5 to show rates, the first non-constant term T_1' (i.e. C_{14}) may be appended, along with R_1', the rate at which intermediate species arrive at $\boxed{M(C_2)_7}$, and R_2', the rate at which intermediate species originating from before $\boxed{M(C_2)_7}$ arrive at $\boxed{M(C_2)_8}$ (Scheme 8).

In an effort to find α' and β' (i.e. the α and β values at C_{14}) and R_1' and R_2', three distinct equations involving the four unknown variables may be identified (note that T_1' is the experimental data point for 1-tetradecene):

$$\beta' R_1' = R_2 \tag{26a}$$

$$\alpha' R_1' + R_2' = R_1 \tag{26b}$$

$$\left(1 - \alpha' - \beta'\right)R_1' = T_1' \tag{26c}$$
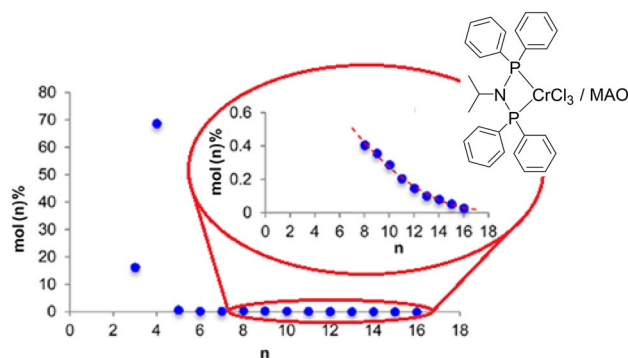
These equations sum to give:

Fig. 16 Selective α-olefin distribution as mol(n)% vs n (units of ethylene) obtained with Cr/$Ph_2PN(^iPr)PPh_2$/MAO [16, 30]. Conditions: 10 µmol Cr, 30 bar, 30 °C, MAO (3 mmol), toluene (100 mL), 30 min. Inset: enlargement of distribution from C_{16+}. Inset: Expanded mol(n)% vs. n for the C_{16}–C_{32} fraction

Fig. 17 Condensed energy profiles for 1-hexene and 1-octene formation from the singly-coordinated chromacyclopentane intermediate 7 [30]. Gaussian09, M06L/quadruple-ζ valence def2-QZVP basis set and SDD ECP on Cr, 6-311 + G(2d,p) basis set on all other atoms
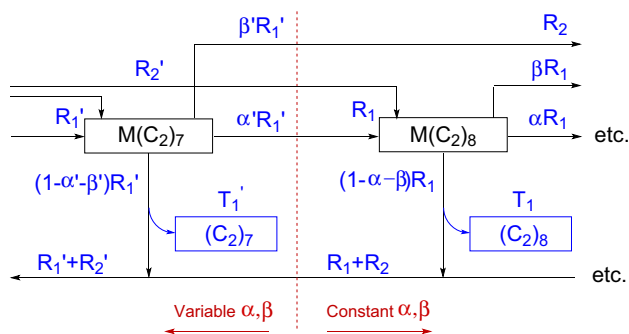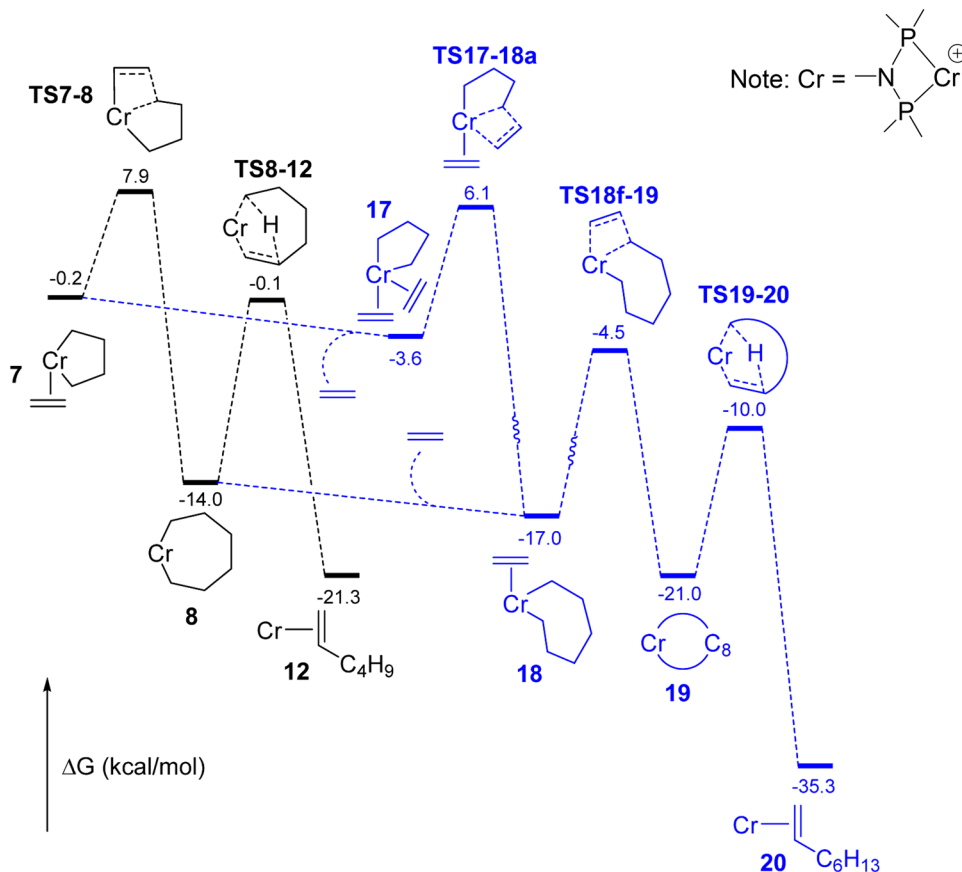
Scheme 8 Catalytic scheme for Fig. 16 at the boundary of the variable α, β and constant α, β regions

$$R'_1 + R'_2 = R_1 + R_2 + T'_1 \tag{26d}$$

Given that there are three distinct equations for four unknowns (α', β', R'_1 and R'_2), a unique solution does not exist in this case. If no further information is available/applied from e.g. theoretical studies, an assumption (such as $\frac{\alpha'}{\beta'} = \frac{\alpha}{\beta}$) is required as a fourth equation to determine unique solutions for the four unknown variables.

# 3 Modelling Non-Steady-State Polymerisation Processes

3.1 Connecting Schulz–Flory Distributions and Poisson Distributions

The mathematics behind Schulz–Flory ethylene oligomer distributions was first accurately described in 1936 [19]. In 1940, Flory went on to give a kinetic derivation of Poisson's equation for polymer distributions obtained from a monofunctional monomer (ethylene oxide) [34]. Yet the mathematical connection between Schulz–Flory distributions and Poisson distributions has not been fully elucidated. In this section, the relationship between the two is made explicit from first principles.

It should be noted that the treatment presented below is described with ethylene as the monomer, but is generally applicable to oligomerisation and polymerisation processes involving the sequential incorporation of monomers in forming linear product chains.

3.1.1 First Principles

The mechanics of a first-order ethylene oligomerisation or polymerisation process whereby propagation proceeds

Scheme 9 Catalytic scheme for first-order propagation

$$\sum_{n=0}^{\infty} M(n) = L \ (units = mol \ dm^{-3})$$

$$k_p, k_e \ units = s^{-1}$$
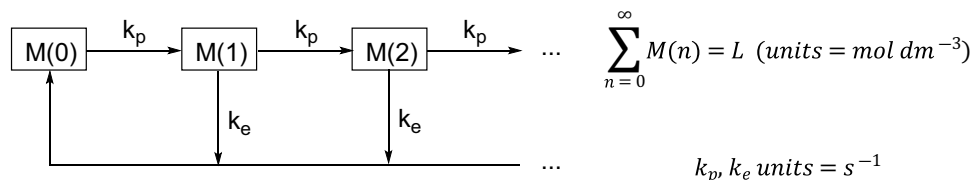
via metal alkyl or metallacyclic species is summarised in Scheme 9. In this model and the following mathematical treatment, we assume that the rate constants k_p and k_e are constant over time and independent of chain length. Furthermore, all active species must start the polymerisation instantaneously and there is no catalyst deactivation.

$M(n)$ represents catalyst intermediates involving n ethylene units (e.g. $M(0) =$ metal hydride species, $M(1) =$ metal ethyl or metallacyclopropane species, $M(2) =$ metal butyl or metallacyclopentane species etc.), k_p is the rate constant of propagation, k_e is the rate constant of elimination, and L is the total precatalyst loading.

A general expression for $M(n)$, as a function of time, may be derived (see SI.5.1):

$$M(n) = \frac{Lk_p^n k_e}{(k_p + k_e)^{(n+1)}} \tag{28}$$

Given that elimination occurs at a constant rate, the interest lies only in the sum of linear alpha olefins of chain length n ethylene units continuously eliminated from t_0 to t_{end}:

$$mol(n)_{t_{end}} = k_e \int_0^{t_{end}} M(n)dt = \frac{Lk_p^n k_e^2 t_{end}}{(k_p + k_e)^{(n+1)}}$$

$$= \frac{Lk_e^2 t_{end}}{k_p}\alpha^{(n+1)} \text{where } \alpha = \frac{k_p}{(k_p + k_e)} \tag{29a}$$

$$M(n)_t = \frac{k_p^n L}{n!\,(k_p + k_e)^{(n+1)}} \left[e^{-(k_p+k_e)t}\left(k_p[(k_p + k_e)t]^n - k_e \sum_{i=1}^{i=n} \frac{n!}{(n-i)!}[(k_p + k_e)t]^{(n-i)} \right) + n!\,k_e \right] \tag{27}$$

$$\underbrace{\phantom{e^{-(k_p+k_e)t}\left(k_p[(k_p + k_e)t]^n - k_e \sum_{i=1}^{i=n} \frac{n!}{(n-i)!}[(k_p + k_e)t]^{(n-i)} \right)}}_{\text{Non-steady-state term}} \quad \underbrace{}_{\text{Steady-state term}}$$

The label "non-steady-state" refers to time dependent terms, whilst the label "steady-state" refers to time independent terms. It is worth noting again that Scheme 9 assumes k_p and k_e are constant over time and independent of $M(n)$, i.e. no distinction in propagation or elimination kinetics is made between the various intermediate groups in the catalytic scheme. In addition, by combining $M(n)$ species in forming the kinetics equations, it is implicitly assumed that a single species within each $M(n)$ group dominates. For instance, the $M(0)$ group includes both metal hydrides with a vacant site and ethylene-associated metal hydrides. This assumption is no longer required for the Schulz–Flory case, given that steady-state kinetics operate.

3.1.2 Derivation of the Schulz–Flory Equation for First-Order Steady-State Oligomerisation

Referring to Scheme 9, the scenario where steady state is achieved from t_0 (i.e. instantaneously from the beginning of reaction) with $k_e \neq 0$ corresponds to the limiting case of first-order steady-state oligomerisation. In such a case, by ignoring non-steady-state terms, Eq. 27 simplifies to:

$$mol(n)\% = \frac{\frac{Lk_e^2 t_{end}}{k_p}\alpha^{(n+1)}}{\frac{Lk_e^2 t_{end}}{k_p}\left[\alpha^2 + \alpha^3 + \alpha^4 + \ldots\right]} = \frac{\alpha^{(n+1)}}{\alpha^2 + \alpha^3 + \alpha^4 + \ldots}$$

$$\alpha^2 + \alpha^3 + \alpha^4 + \ldots = \frac{\alpha^2}{(1-\alpha)} \text{when} |\alpha| < 1, \text{so}:$$

$$mol(n)\% = \frac{(1-\alpha)}{\alpha^2}\alpha^{(n+1)} = (1-\alpha)\alpha^{(n-1)} \tag{29b}$$

Equation 29a is the unnormalised Schulz–Flory equation, and Eq. 29b is the normalised Schulz–Flory equation. Note in Eq. 29a that the total mol of oligomers produced during the reaction time $R = L\alpha k_e t_{end}$. Given that both $\frac{Lk_e^2 t_{end}}{k_p}$ (where L and t_{end} are known) and α may be fitted, k_p and k_e may be inferred.

3.1.3 Derivation of Poisson's Equation for First-Order Living Polymerisation

Referring again to Scheme 9, setting $k_e = 0$, i.e. there is no chain termination process, corresponds to the limiting case of first-order non-steady-state living polymerisation. In such a case, Eq. 27 simplifies to:

$$M(n)_t = \frac{L}{n!k_p}\left[e^{-k_p t}\left(k_p^{(n+1)}t^n\right)\right] \leftrightarrow M(n)_t = \frac{L(k_p t)^n}{n!}e^{-k_p t}$$

(30)

Given that no termination occurs throughout, the interest lies only in the distribution of intermediate species at t_{end} (i.e. the end of reaction), which would give n-alkene products on thermal termination (as per the INEOS (Ethyl) process [8]) or n-alkane products upon hydrolysis. At this point:

$$M(n)_{t_{end}} = mol(n)_{t_{end}} = \frac{L(k_p t_{end})^n}{n!}e^{-k_p t_{end}} = \frac{L\lambda^n}{n!}e^{-\lambda} \quad (31a)$$

$$mol(n)_{t_{end}}\% = \frac{\frac{L\lambda^n}{n!}e^{-\lambda}}{\sum_{n=1}^{n=\infty}\frac{L\lambda^n}{n!}e^{-\lambda}} = \frac{L\lambda^n e^{-\lambda}}{n!Le^{-\lambda}\sum_{n=1}^{n=\infty}\frac{\lambda^n}{n!}} = \frac{\lambda^n e^{-\lambda}}{n!e^{-\lambda}(e^{\lambda}-1)} = \frac{\lambda^n e^{-\lambda}}{n!(1-e^{-\lambda})}$$

(31b)

Equation 31a is Poisson's equation scaled by the precatalyst loading L, and Eq. 31b is Poisson's equation scaled by the factor $\left(1-e^{-\lambda}\right)^{-1}$ (which quickly approaches 1 as λ increases). Note that λ is the mean number of ethylene units per chain. Given that λ may be fitted (where t_{end} is known), k_p may be inferred.

3.2 Non-Steady-State Living Polymerisation with Catalysed Chain Growth

In 1952, Ziegler et al. reported the *Aufbaureaktion* involving the formation of long chain trialkylaluminium species via stepwise insertion of ethylene monomers into Al–C bonds (starting with triethylaluminium, for instance) [35]. The effect of transition metals, such as colloidal Ni, in suppressing chain growth in the *Aufbaureaktion* to selectively form 1-butene was subsequently discovered [36]. This prompted a screening of the d-block transitional metals for other metal effects and, in the case of titanium, this led to the first reported transition metal catalysed ethylene polymerisation [37, 38].

In their early work, Ziegler et al. described the process as a transition metal catalysed *Aufbaureaktion*, with the alkylaluminium functioning as the polymerisation catalyst and the transition metal compound functioning as the co-catalyst [37]. Later it was found that the polymer chain grows on the transition metal centre, rather than on aluminium. More recently however, several processes have been reported where the polymer chain is transferred during the course of the reaction from a transition metal to a main group metal such as aluminium, magnesium or zinc [39–44]. If this chain transfer is very fast and reversible, then it appears as if the polymer chains grow on the main group metal centres instead. Such a reaction is generally described as a catalysed chain growth (CCG) process or a coordinative chain-transfer polymerisation (CCT), or, to employ the original terminology, a transition metal catalysed *Aufbaureaktion* [44–46].

Tremendous advances have been made in CCG during the past 2 decades, but the mathematics of generating product distributions via CCG has not yet been reported. Such a treatment from first principles is presented here and then applied next.

3.2.1 First Principles

Scheme 10 summarises the mechanics of a first-order ethylene oligomerisation or polymerisation process whereby

Scheme 10 Catalytic scheme for first-order propagation with chain transfer

$M(n), CT(n)$ *units* $= mol\ dm^{-3}$

All k_p, k_e *units* $= s^{-1}$

All k_{ct} *units* $= mol^{-1}dm^3 s^{-1}$
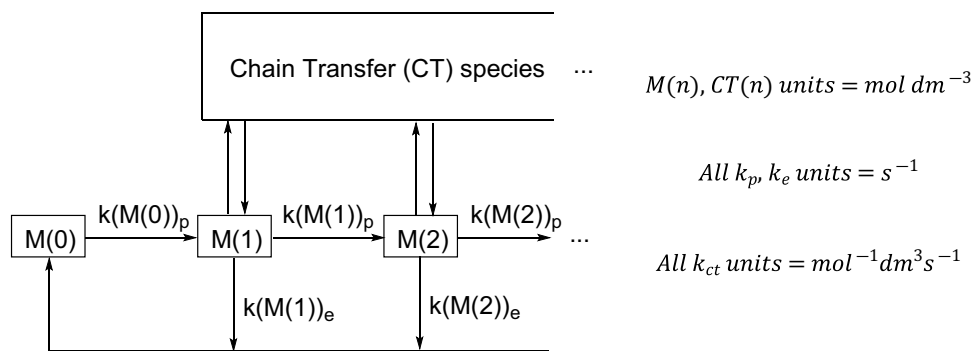
propagation proceeds via metal alkyl or metallacyclic species, and chain transfer to and amongst a population of non-propagating agents is possible. A similar caveat as in Sect. 3.1 applies in that in this model and the following mathematical treatment, we assume that the rate constants k_p, k_e and k_{ct} are constant over time and independent of chain length. Furthermore, all active species must start the polymerisation instantaneously and there is no catalyst deactivation.

$M(n)$ represents transition metal intermediates involving n ethylene units, $CT(n)$ represents the population of chain transfer species bearing an alkyl chain of length n ethylene units, $k(M(n))_p$ is the rate constant of propagation for $M(n)$, $k(M(n))_e$ is the rate constant of elimination for $M(n)$, and k_{ct}'s are rate constants of chain transfer between species.

Scheme 10 is not labelled with individual k_{ct}'s given the general nature of the present treatment.

It is possible to show (see SI.5.2) that:

$$\frac{d}{dt}M(n)_t = k(M(n-1))_p M(n-1)_t - \left[k(M(n))_p + k(M(n))_e\right]M(n)_t$$

(32)

This expression for change does not show dependence on chain transfer terms. In other words, the underlying $M(n)$ system drives towards the distribution that it would adopt in the absence of chain transfer agent. However, the nature of instantaneous steady state for CT species slows down the overall rate at which the $M(n)$ system evolves vs. the case with no chain transfer.

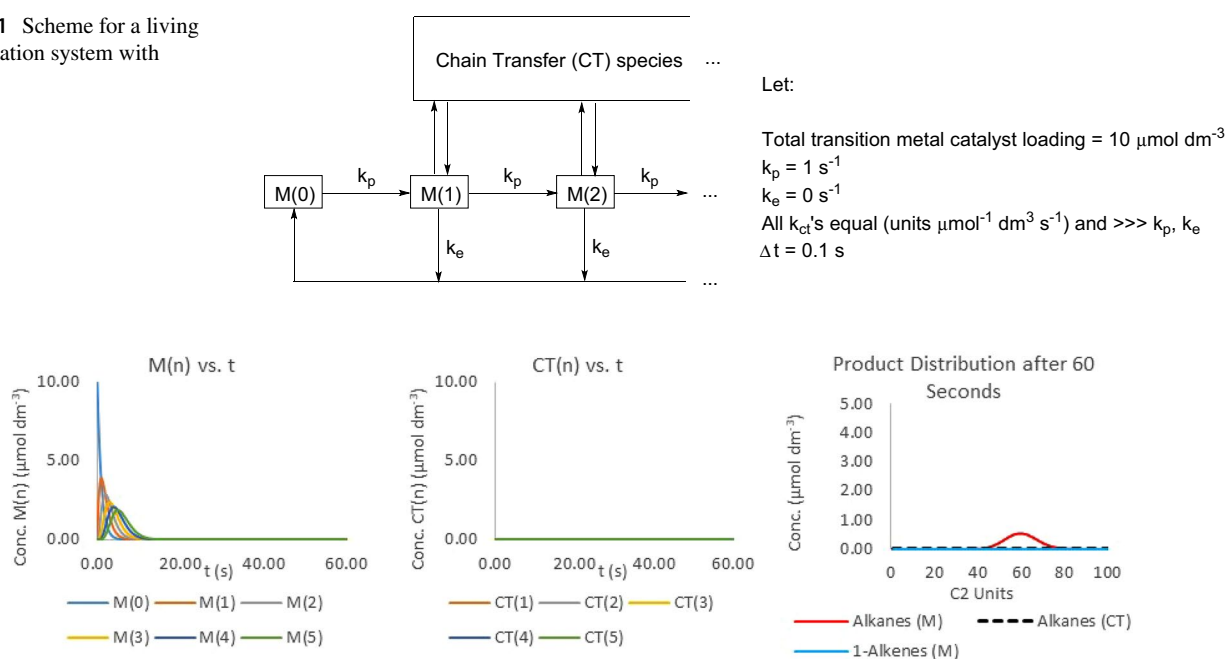Scheme 11 Scheme for a living polymerisation system with CCG

Fig. 18 System evolution and product distribution with CT agent loading $=0$ µmol dm^{-3} (0 eqv. vs. transition metal catalyst). Note: M(n) and CT(n) up to n $=5$ illustrated left and centre, all n captured right

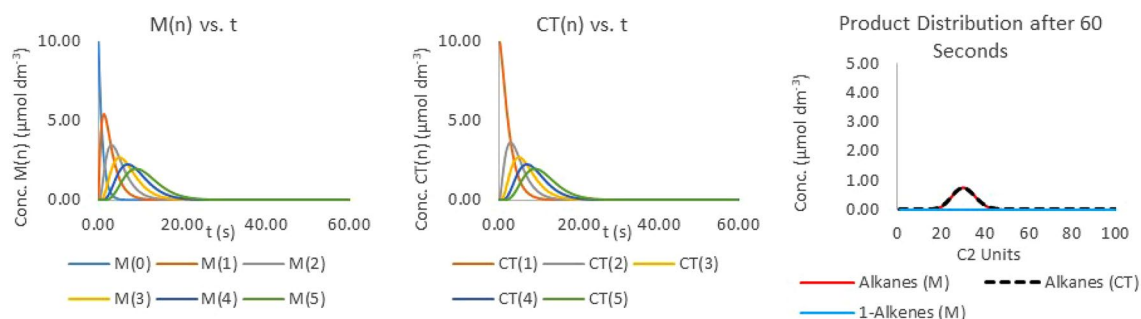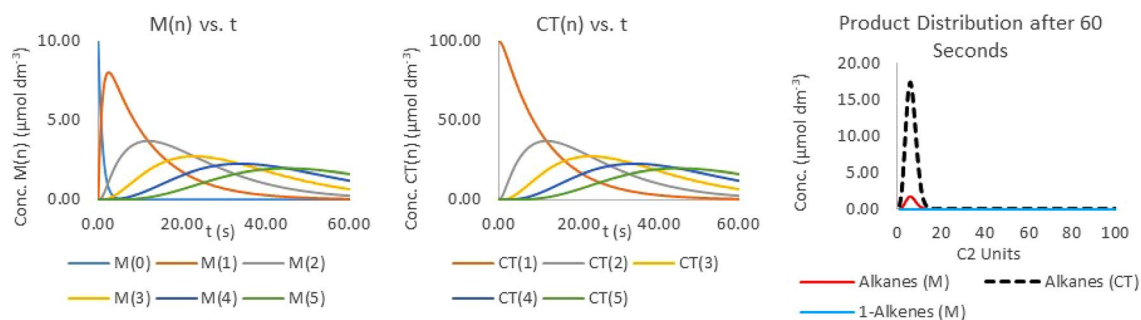Fig. 19 System evolution and product distribution with CT agent loading $=10$ µmol dm^{-3} (1 eqv. vs. transition metal catalyst). Note: M(n) and CT(n) up to n $=5$ illustrated left and centre, all n captured right

Fig. 20 System evolution and product distribution with CT agent loading = 100 μmol dm^{-3} (10 eqv. vs. transition metal catalyst). Note: M(n) and CT(n) up to n = 5 illustrated left and centre, all n captured right

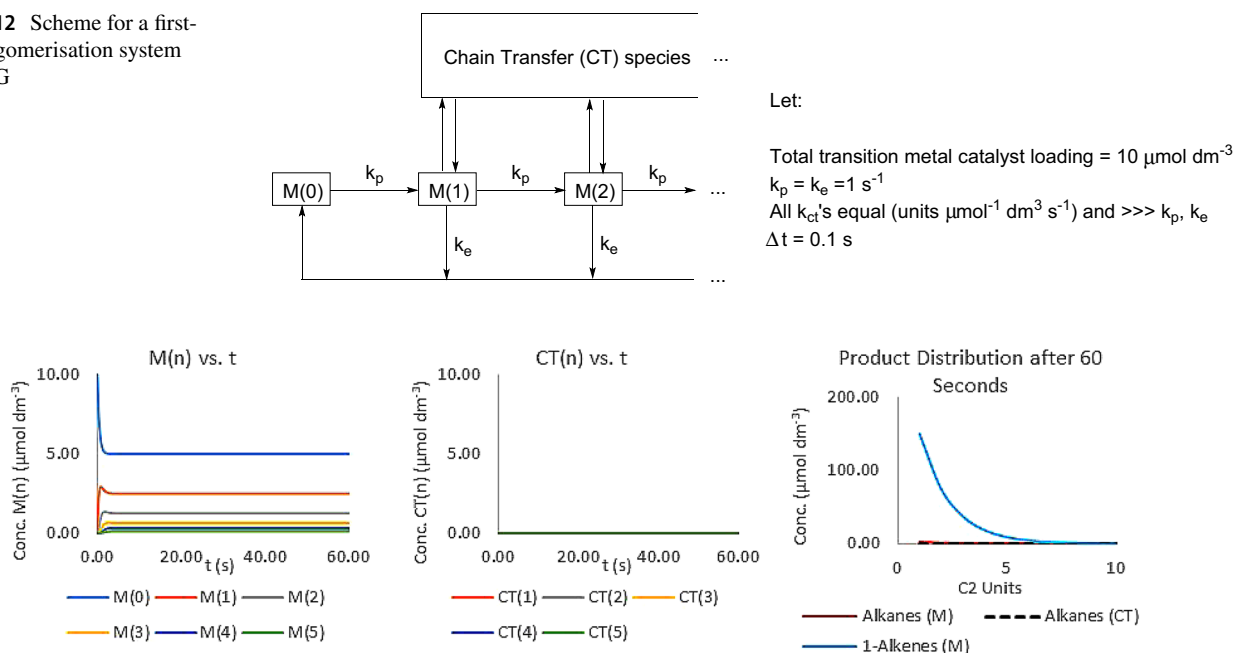**Scheme 12** Scheme for a first-order oligomerisation system with CCG

Let:

Total transition metal catalyst loading = 10 μmol dm^{-3}
$k_p = k_e = 1$ s^{-1}
All k_{ct}'s equal (units μmol^{-1} dm^3 s^{-1}) and >>> k_p, k_e
$\Delta t = 0.1$ s

Fig. 21 System evolution and product distribution with CT agent loading = 0 μmol dm^{-3} (0 eqv. vs. transition metal catalyst). Note: M(n) and CT(n) up to n = 5 illustrated left and centre, all n captured right

3.2.2 Numerical Simulations

Two illustrative examples are provided to demonstrate the preceding mathematics. Numerical simulations of evolving oligomerisation or polymerisation systems which involve chain transfer, as per Scheme 10, are possible with Microsoft Excel (see SI.5.3 for details).

3.2.3 Illustrative Example 1: Living Polymerisation with Catalysed Chain Growth

See Scheme 11, Figs. 18, 19, 20.

3.2.4 Illustrative Example 2: First-Order Oligomerisation with Catalysed Chain Growth

See Scheme 12, Figs. 21, 22, 23.

3.2.5 The Fitting Process

The preceding discussion demonstrated how Poisson distributions or Schulz–Flory distributions are still generated for first-order systems involving CCG. Section 2.1 provided the details for modelling first-order steady state oligomerisation systems, which by extension may be applied to first-order oligomerisation systems involving CCG. Section 3.1 gave a derivation to the Poisson distribution for living polymerisation systems, ending at Eqs. 31a and 31b.
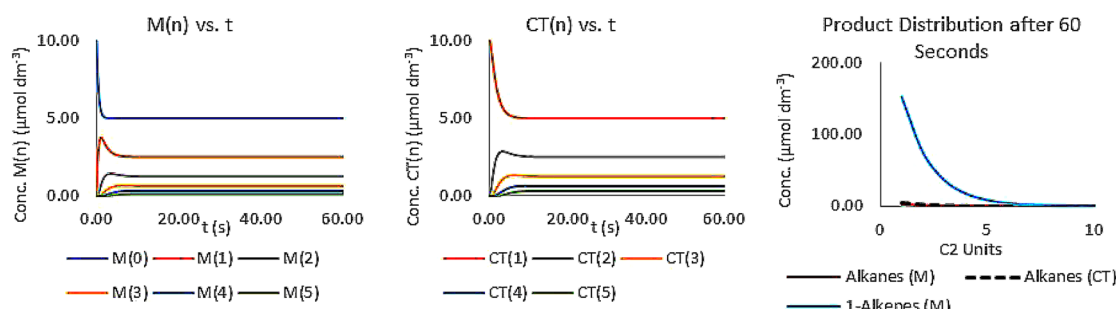
Fig. 22 System evolution and product distribution with CT agent loading = 10 μmol dm^{-3} (1 eqv. vs. transition metal catalyst). Note: M(n) and CT(n) up to n = 5 illustrated left and centre, all n captured right

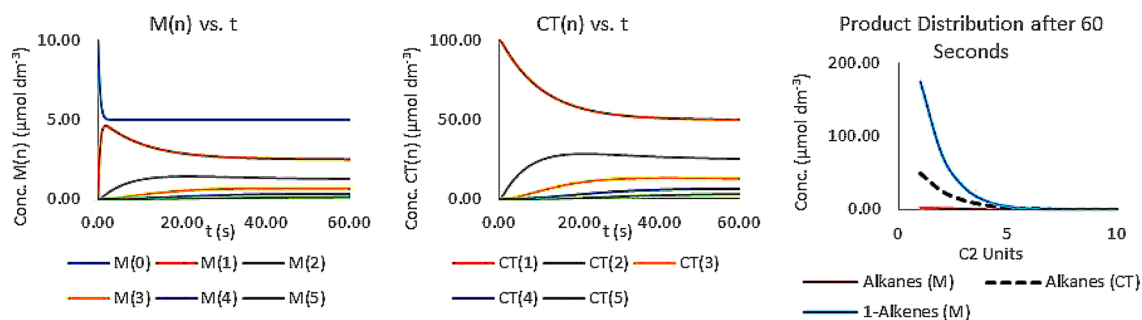**Fig. 23** System evolution and product distribution with CT agent loading = 100 μmol dm^{-3} (10 eqv. vs. transition metal catalyst). Note: M(n) and CT(n) up to n = 5 illustrated left and centre, all n captured right

When Eqs. 31a and 31b are applied to living polymerisation systems with CCG, in order to capture all intermediate alkyl chains, *L* is now defined as:

$$L = \textit{Transition metal catalyst loading}$$
$$+ (\textit{CT loading})(\textit{Alkyl chains per CT species}) \quad (33)$$

Furthermore, k_p may now be interpreted as the effective propagation rate constant for the entire system. The process for modelling living polymerisation systems with CCG is described next, along with derivations of the experimentally-relevant metrics M_n, M_w and *PDI*. For illustration, a comparison is also made between an experimentally determined result vs. the fitted data.

3.2.6 Back-Solving to Determine *L* and λ, and Checking for the Best Fit

In practice, the $mol(n)_{t_{end}}$ values in Eq. 31a are known (i.e. mol of each oligomer produced during the reaction time), and the aim is to find *L* and λ. See SI.5.4 for a discussion on the method used to determine α and *R*, as well as a checking method to determine that the best fit has been found.

3.2.7 Derivations of Further Experimentally-Relevant Metrics

For a distribution of *n*-alkenes, the following expressions can be derived (see SI.5.5 and SI.5.6):

$$wt(n)_{t_{end}}\% = \frac{n\lambda^{n-1}e^{-\lambda}}{n!} \quad (34)$$

$$M_{n_{t_{end}}} = (RFMC_2H_4)\lambda(1 - e^{-\lambda})^{-1} \quad (35)$$

$$M_{w_{t_{end}}} = (RFMC_2H_4)(\lambda + 1) \quad (36)$$

$$PDI = \frac{M_{w_{t_{end}}}}{M_{n_{t_{end}}}} = \frac{(\lambda + 1)(1 - e^{-\lambda})}{\lambda} \quad (37)$$

As λ increases, the factor $(1 - e^{-\lambda})$ approaches 1. Under such circumstances, Eqs. 35 and 37 simplify.

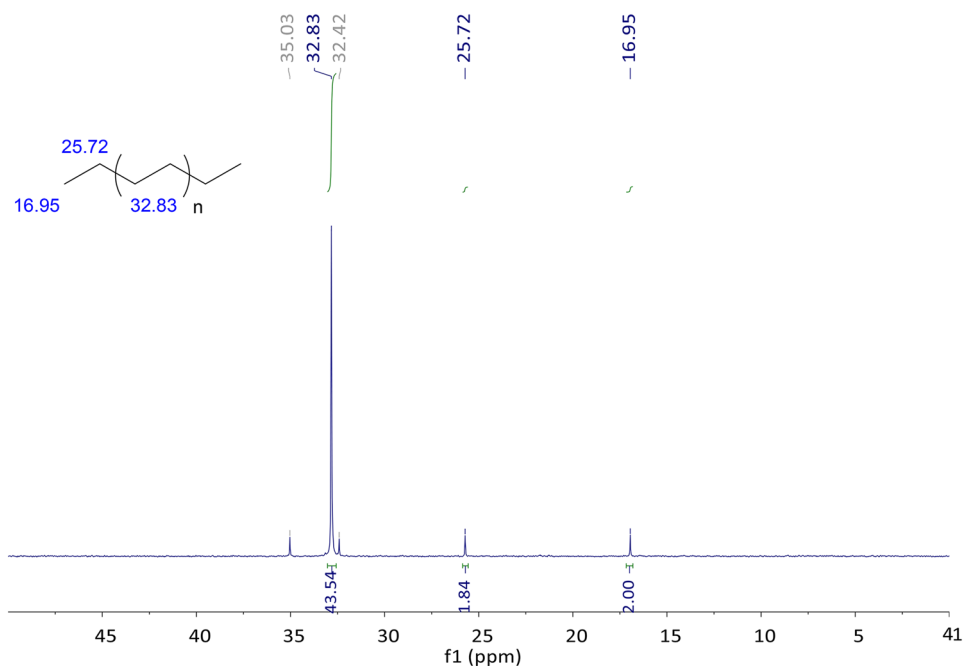$$M_{n_{t_{end}}} \rightarrow (RFMC_2H_4)\lambda \quad (38)$$

Fig. 24 Quantitative $^{13}C\{^1H\}$ NMR spectrum of n-alkane oligomer product (solvent: d_2-1,1,2,2-tetrachloroethane/1,2,4-trichlorobenzene 50/50 v/v), 100 MHz, 100 °C

$$PDI \rightarrow \frac{(\lambda + 1)}{\lambda} = 1 + \frac{1}{\lambda} \rightarrow 1 \qquad (39)$$

With high values of λ, *PDI* tends towards unity, as per the literature [47].

3.2.8 Comparison of an Experimentally Determined Result vs. Fitted Data

CCG polymerisations have been performed, using $ZnEt_2$ as the CT agent with 2,6-diacetylpyridinebis(2,6-diisopropylanil)$FeCl_2$/MAO (experimental details, see SI.5.7). Termination of the polymerisation reaction is carried out by hydrolysis, resulting in a mixture of long-chain alkanes. Given a highly symmetric Poisson distribution of the resulting n-alkane oligomers, quantitative $^{13}C\{^1H\}$ NMR analysis may be used to estimate the mean chain length by comparing integrals for CH_3 with those for CH_2. For the given experiment, quantitative $^{13}C\{^1H\}$ NMR spectroscopy gives a CH_3:CH_2 ratio of 2:45.38, implying a mean chain length between 46 and 48 carbons (see Fig. 24).
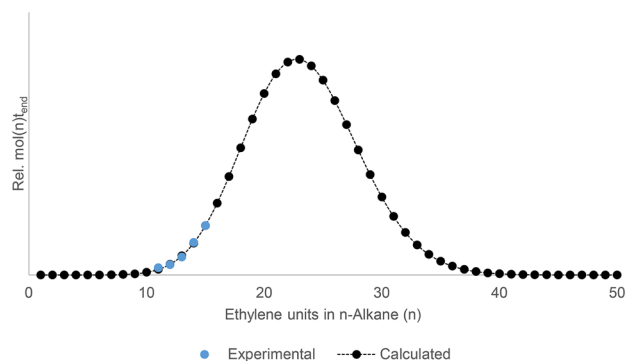

Fig. 25 Modelled outputs (see Table 5) vs. experimental GC data

Experimental characterisation of the alkane distribution in such mixtures is non-trivial. The average molecular weight is typically too low for accurate GPC analysis, and the longer alkanes are often insufficiently volatile for conventional quantitative GC-FID analysis. Only the first part of the n-alkane oligomer distribution is usually

Table 5 Modelled outputs using experimental GC data

λ	23.3
k_p/s^{-1}	6.5E−03
Mean chain length (No. of carbons)	46.6
$M_n/g\ mol^{-1}$	655.15
$M_w/g\ mol^{-1}$	683.11
$Đ_M$	1.04
Mol% (C_2 to C_∞)	$\frac{(23.3^n)*(e^{-23.3})}{n!*(1-e^{-23.3})}$
Wt% (C_2 to C_∞)	$\frac{(23.3^n)*(e^{-23.3})*[n(RFMC2H4)+(RAM2H)]}{n!*[(RFMC2H4)*23.3+(RAM2H)*(1-e^{-23.3})]}$
R^2 fit	0.996
Fit L, λ/mmol^2	0.001
δ(Fit L, λ)/δL/mmol	0.00000
δ(Fit L, λ)/$\delta\lambda$/mmol^2	0.00000

quantifiable via GC. These signals have been used here as inputs for the fitting model. Following the procedure previously described in this sub-section, the values in Table 5 are found.

3.2.9 Model Outputs

There is a high degree of correlation between calculated and experimental values in Table 5 (goodness of fit $R^2 = 0.996$), and the calculated mean chain length of 46.6 carbons is within the range previously specified by quantitative $^{13}C\{^1H\}$ NMR spectroscopy. This method therefore allows the entire product distribution to be determined from a subset of experimental data obtained by GC analysis.

4 Conclusions and Summary

A variety of different distributions—including Schulz–Flory, alternating, selective-LAO, and Poisson distributions—of linear hydrocarbon products can be obtained from ethylene oligomerisation and polymerisation processes. Oligomerisation processes are steady-state in nature, and can be mathematically described using recurrence relations. First order oligomerisation processes propagate via sequential single-insertions of ethylene, whereas second order oligomerisation processes propagate via sequential single- and double-insertions of ethylene. From an analytical point of view, an important consideration with regards to second order processes is the degree of alternation exhibited by a given distribution, which is generally more pronounced at higher ethylene pressure. The degree of alternation for a particular distribution may be defined as the relative ratio of alternating vs. Schulz–Flory character. An overview of the key analytical results from first order and second order processes with constant probabilities of propagation is given in Table 6.

Examples of first order and second order oligomerisation processes which involve varying probabilities of propagation have been identified from the literature. Such systems include selective oligomerisation catalysts such as the well-known chromium-based tetramerisation catalysts. An analytical method is available for handling first order processes with varying probabilities of propagation. However, there is a theoretical limitation to a similar approach for analogous second order processes.

The connection between distributions from first order steady-state oligomerisations (Schulz–Flory) and first order non-steady-state polymerisations (Poisson) is made through a consideration of kinetic differential equations. The addition of a chain transfer agent (e.g. $ZnEt_2$) to such systems results in a slowing down of the overall propagation rate. Accurate modelling of a CCG polymerisation system featuring $ZnEt_2$ as the CT agent has been achieved, allowing for the derivation of several key mechanistic parameters.

The mathematics of ethylene oligomerisation presented here can be easily applied to other systems where chain growth proceeds through an oligomerisation process. Examples of such systems would be the oligomerisation of higher α-olefins to poly(α-olefin) oils, the dehydropolymerisation of aminoboranes, chain growth reactions in the Fischer–Tropsch process or the formation of oligonucleotides. By fitting the experimental results to the formulas described herein for the various oligomerisation scenarios, valuable information may be extracted regarding the underlying reaction mechanisms of the oligomerisation process.

Table 6 Key analytical results from 1st order and 2nd order processes with constant probabilities of propagation

	First order (Schulz–Flory)	Second order (Alternating)
Recurrence relation type	First-order linear homogeneous recurrence relation with constant coefficients	Second-order linear homogeneous recurrence relation with constant coefficients
Relation	$T_{n+1} = \alpha T_n$	$T_{n+2} = \alpha T_{n+1} + \beta T_n$
General solution	$T_n = c r^n$ $r = \alpha$ $c = \frac{(1-\alpha)}{\alpha} R$ α = propagation probability $(1-\alpha)$ = elimination probability R = total amount in mol of oligomer produced during reaction time	$T_n = c_1 r_1^n + c_2 r_2^n$ $r_1 = \frac{\alpha + \sqrt{\alpha^2 + 4\beta}}{2}$ $r_2 = \frac{\alpha - \sqrt{\alpha^2 + 4\beta}}{2}$ $c_1 = \frac{(1-\alpha-\beta)(R_1 r_1 + R_2)}{r_1(r_1 - r_2)}$ $c_2 = \frac{(1-\alpha-\beta)(R_1 r_2 + R_2)}{r_2(r_2 - r_1)}$ α/β = propagation probability via single-/double-insertion $(1-\alpha-\beta)$ = elimination probability $R_1 + R_2$ = total amount in mol of oligomer produced during reaction time
$mol(n)$, $mol(n)\%$ and $wt(n)\%$ equations	$mol(n) = c r^n = (1-\alpha)\alpha^{n-1} R$ $mol(n)\% = (1-\alpha)\alpha^{n-1}$ $wt(n)\% = n(1-\alpha)^2 \alpha^{n-1}$	$mol(n) = c_1 r_1^n + c_2 r_2^n$ $mol(n)\% = \frac{c_1 r_1^n + c_2 r_2^n}{R_1 + R_2}$ $= \frac{c_1 r_1^n + c_2 r_2^n}{\frac{c_1 r_1}{1-r_1} + \frac{c_2 r_2}{1-r_2}}$ $wt(n)\% = \frac{n(c_1 r_1^n + c_2 r_2^n)}{\frac{c_1 r_1}{(1-r_1)^2} + \frac{c_2 r_2}{(1-r_2)^2}}$
M_n, M_w and PDI equations	$M_n = \frac{(RFM C_2 H_4)}{(1-\alpha)}$ $M_w = \frac{(RFM C_2 H_4)(1+\alpha)}{(1-\alpha)}$ $PDI = (1+\alpha)$	$M_n = \frac{(RFM C_2 H_4)}{\frac{c_1 r_1}{1-r_1} + \frac{c_2 r_2}{1-r_2}} \left[\frac{c_1 r_1}{(1-r_1)^2} + \frac{c_2 r_2}{(1-r_2)^2} \right]$ $M_w = \frac{(RFM C_2 H_4)}{\frac{c_1 r_1}{(1-r_1)^2} + \frac{c_2 r_2}{(1-r_2)^2}} \left[\frac{c_1 r_1 (1+r_1)}{(1-r_1)^3} + \frac{c_2 r_2 (1+r_2)}{(1-r_2)^3} \right]$ $PDI = \frac{py + qx}{[py^2 + qx^2]^2} \left[py^3(2-x) + qx^3(2-y) \right]$ $p = c_1 r_1$ $q = c_2 r_2$ $x = 1 - r_1$ $y = 1 - r_2$
Further equations	–	$Deg.\ of\ Alt. = \frac{+\sqrt{\left(r_2 + \frac{R_2}{R_1}\right)^2}(1-r_1)}{\left(r_1 + \frac{R_2}{R_1}\right)(1+r_2)}$ $\frac{\beta}{\alpha} = \frac{P_{et}}{g_1 + g_2 P_{et}}$ g_1, g_2 = constants across P_{et}

Compliance with Ethical Standards

Conflict of interest The authors declare that they have no conflict of interest.

References

1. Breuil P-AR, Magna L, Olivier-Bourbigou H (2015) Catal Lett 145(1):173–192
2. Forestière A, Olivier-Bourbigou H, Saussine L (2009) Oil Gas Sci. Technol Rev l'IFP 64(6):649–667
3. Olivier-Bourbigou H, Forestière A, Saussine L, Magna L, Favre F, Hugues F (2010) Oil Gas Eur Mag 36:97
4. Ring K-L, DeGuzman M (2017) Chemical economics handbook: linear alpha-olefins, IHS Chemical
5. Process Economics Program (PEP) (2016) Wide range linear alpha olefin processes & on-purpose linear alpha olefin processes, PEP CR001 & CR002 Prospectus, IHS Chemical
6. Sydora O (2019) Organometallics 38:997–1010
7. Keim W (2013) Angew Chem Int Ed 52(48):12492–12496
8. Greiner EOC, Inoguchi Y (2010) Chemical economics handbook: linear-alpha olefins, IHS Chemical
9. McGuinness DS (2011) Chem Rev 111(3):2321–2341
10. Van Leeuwen PWNM, Clément ND, Tschan MJL (2011) Coord Chem Rev 255(13–14):1499–1517
11. Chen Y, Zuo W, Hao P, Zhang S, Gao K, Sun W-H (2008) J Organomet Chem 693(4):750–762
12. Luo W, Li A, Liu S, Ye H, Li Z (2016) Organometallics 35(17):3045–3050
13. Tenza K, Hanton MJ, Slawin AMZ (2009) Organometallics 28(16):4852–4867
14. Liu S, Pattacini R, Braunstein P (2011) Organometallics 30(13):3549–3558
15. Tomov AK, Chirinos JJ, Long RJ, Gibson VC, Elsegood MRJ (2006) J Am Chem Soc 128(24):7704–7705
16. Britovsek GJP, Malinowski R, McGuinness DS, Nobbs D, Tomov AK, Wadsley AW, Young CT (2015) ACS Catal 5(11):6922–6925
17. Tomov AK, Nobbs JD, Chirinos JJ, Saini PK, Malinowski R, Ho SKY, Young CT, McGuinness DS, White AJP, Elsegood MRJ, Britovsek GJP (2017) Organometallics 36(3):510–522
18. Schulz GVZ (1935) Phys Chem Abt B 1935(30):379–398
19. Flory PJ (1936) J Am Chem Soc 58(7):1877–1885
20. Britovsek GJP, Mastroianni S, Solan GA, Baugh SPD, Redshaw C, Gibson VC, White AJP, Williams DJ, Elsegood MRJ (2000) Chem. A 6(12):2221–2231
21. Briggs JR (1989) J Chem Soc Chem Commun 11:674
22. Tomov AK, Gibson VC, Britovsek GJP, Long RJ, Van Meurs M, Jones DJ, Tellmann KP, Chirinos JJ (2009) Organometallics 28(24):7033–7040
23. Agapie T, Labinger JA, Bercaw JE (2007) J Am Chem Soc 129(46):14281–14295
24. Tomov AK, Chirinos JJ, Jones DJ, Long RJ, Gibson VC (2005) J Am Chem Soc 127(29):10166–10167
25. Ystenes M (1991) J Catal 129:383
26. Marques MM, Dias AR, Costa C, Lemos F, Ramôa Ribeira F (1997) Polym Int 43:77–85
27. Matos I, Zhang Y, Lemos MANDA, Freire F, Fonseca IF, Marques MM, Lemos FJ (2004) Polym Sci A 42(14):3464–3472
28. Mark Kelly W, Wang S, Collins S (1997) Macromolecules 30(11):3151–3158
29. McGuinness DS, Suttil JA, Gardiner MG, Davies NW (2008) Organometallics 27(16):4238–4247
30. Britovsek GJP, McGuinness DS, Wierenga TS, Young CT (2015) ACS Catal 5(7):4152–4166
31. McGuinness DS, Chan B, Britovsek GJP, Yates BF (2014) Aust J Chem 67(10):1481–1490
32. Britovsek GJP, McGuinness DS, Tomov AK (2016) Catal Sci Technol 6:8234–8241
33. Britovsek GJP, McGuinness DS (2016) Chem-Eur J 22:16891–16896
34. Flory PJ (1940) J Am Chem Soc 62(6):1561–1565
35. Ziegler K, Gellert HG, Kühlhorn H, Martin H, Meyer K, Nagel K, Sauer H, Zosel K (1952) Angew Chem 64:323–329
36. Ziegler K, Gellert HG, Holzkamp E, Wilke G (1954) Brennstoff-Chem 35:321–352
37. Ziegler K, Holzkamp E, Breil H, Martin H (1955) Angew Chem Int Ed 67:541–547
38. Sauter DW, Taoufik M, Boisson C (2017) Polymers 9:185
39. Lehmkuhl H, Olbrysch O (1975) Eur J Org Chem 6:1162–1175
40. Samsel EG (1993) EP 0539876
41. Samsel EG, Eisenberg DC (1993) EP 0574854
42. Pelletier JF, Bujadoux K, Olonde X, Adisson E, Mortreux A, Chenal T (1998) US 5779942
43. Valente A, Mortreux A, Visseaux M, Zinck P (2013) Chem Rev 113:3836–3857
44. Britovsek GJP, Cohen SA, Gibson VC, Maddox PJ, van Meurs M (2002) Angew Chem Int Ed 41(3):489–491
45. Britovsek GJP, Cohen SA, Gibson VC, van Meurs M (2004) J Am Chem Soc 126(34):10701–10712
46. Sita L (2009) Angew Chem Int Ed 48(14):2464–2472
47. Tobita H (2016) Ullmann's polymers and plastics: products and processes, vol 1. Wiley, Hoboken, p 265